

NPS ARCHIVE
1964
MORELAND, F.

SOLUTION OF THE SINGLE BLOW PROBLEM
WITH LONGITUDINAL CONDUCTION BY
NUMERICAL INVERSION OF LAPLACE
TRANSFORMS

FLOYD E. MORELAND

Library
U. S. Naval Postgraduate School
Monterey, California

SOLUTION OF THE SINGLE BLOW PROBLEM WITH LONGITUDINAL
CONDUCTION BY
NUMERICAL INVERSION OF LAPLACE TRANSFORMS

* * * * *

Floyd E. Moreland



SOLUTION OF THE SINGLE BLOW PROBLEM WITH LONGITUDINAL
CONDUCTION BY
NUMERICAL INVERSION OF LAPLACE TRANSFORMS

by

Floyd E. Moreland
//
Lieutenant, United States Navy

Submitted in partial fulfillment of
the requirements for the degree of

MASTER OF SCIENCE
IN
MECHANICAL ENGINEERING

United States Naval Postgraduate School
Monterey, California

1 9 6 4

NPS Archive

1964

Moreland, F.

~~11/2/17~~

Library
U. S. Naval Postgraduate School
Monterey, California

SOLUTION OF THE SINGLE BLOW PROBLEM WITH LONGITUDINAL

CONDUCTION BY

NUMERICAL INVERSION OF LAPLACE TRANSFORMS

by

Floyd E. Moreland

This work is accepted as fulfilling
the thesis requirements for the degree of

MASTER OF SCIENCE

IN

MECHANICAL ENGINEERING

from the

United States Naval Postgraduate School

ABSTRACT

A system of two partial differential equations represents the transient heat transfer behavior of compact heat exchanger surfaces when subjected to a step change in fluid temperature. A solution is presented for this system which includes the effects of longitudinal thermal heat conduction. Also presented are the solutions for the two limiting cases of zero and infinite longitudinal conduction. The numerical results have been compared to those of C. P. Howard indicating a significant decrease in computational time and an increase in accuracy of results. The revised curves of maximum slope of fluid temperature versus NTU should be of practical value in the evaluation of heat-transfer data obtained by transient testing of compact heat exchanger surfaces. An unusual combination of mathematical techniques is presented for the solution of a boundary value problem involving partial differential equations. The solution combines the application of Laplace transformation with a numerical technique developed by H. Hurwitz, Jr., and P. F. Zweifel, and adapted by L. A. Schmittroth for the inversion of Laplace transforms. This technique greatly expands the number of cases to which Laplace transforms may be successfully applied.

ACKNOWLEDGMENTS

I would like to express my appreciation to my thesis advisor, Dr. U. R. Kodres, Associate Professor, Department of Mathematics and Mechanics, U. S. Naval Postgraduate School, for outlining the mathematical techniques applied to this solution, and for his excellent guidance in the development of the computer programs required. As a result of his active support, the computer solutions obtained are more accurate and the computation time required is considerably less.

I would also like to thank Mr. C. P. Howard, Gas Turbine Division, Code 645, Bureau of Ships, for his advice and guidance during my preliminary investigation of the single blow problem, and for the use of his computer solutions.

CHAPTER I

The first part of the book is devoted to a general survey of the history of the subject. It begins with a brief account of the early attempts to explain the origin of life, and then proceeds to a more detailed examination of the various theories which have been advanced. The author then discusses the evidence in support of each theory, and finally arrives at his own conclusions. The second part of the book is devoted to a more detailed examination of the various theories which have been advanced. The author then discusses the evidence in support of each theory, and finally arrives at his own conclusions. The third part of the book is devoted to a more detailed examination of the various theories which have been advanced. The author then discusses the evidence in support of each theory, and finally arrives at his own conclusions. The fourth part of the book is devoted to a more detailed examination of the various theories which have been advanced. The author then discusses the evidence in support of each theory, and finally arrives at his own conclusions. The fifth part of the book is devoted to a more detailed examination of the various theories which have been advanced. The author then discusses the evidence in support of each theory, and finally arrives at his own conclusions. The sixth part of the book is devoted to a more detailed examination of the various theories which have been advanced. The author then discusses the evidence in support of each theory, and finally arrives at his own conclusions. The seventh part of the book is devoted to a more detailed examination of the various theories which have been advanced. The author then discusses the evidence in support of each theory, and finally arrives at his own conclusions. The eighth part of the book is devoted to a more detailed examination of the various theories which have been advanced. The author then discusses the evidence in support of each theory, and finally arrives at his own conclusions. The ninth part of the book is devoted to a more detailed examination of the various theories which have been advanced. The author then discusses the evidence in support of each theory, and finally arrives at his own conclusions. The tenth part of the book is devoted to a more detailed examination of the various theories which have been advanced. The author then discusses the evidence in support of each theory, and finally arrives at his own conclusions.

TABLE OF CONTENTS

Section	Title	Page
1.	Introduction	1
2.	Mathematical Technique	6
3.	Solution	7
4.	Computer Program	20
5.	Presentation of Results	23
6.	Discussion of Results	31
7.	Conclusions and Recommendations	34
8.	Bibliography	38
Appendix I	Solution for Zero and Infinite Longitudinal Conduction	40
Appendix II	Program Listings and Flow Diagrams	48



LIST OF ILLUSTRATIONS

Figure		Page
1.	NTU versus Maximum Slope	3
2.	Error Magnification Factor versus NTU	4
3.	Comparison of SLO3 and SLO2 versus G	14
4.	-VR or VI versus y	16
5.	SLO2 and SLO4 versus G, NTU = 20, $\bar{\lambda} = 0.0$	27
6.	SLO2 and SLO4 versus G, NTU = 2, $\bar{\lambda} = 0.0$	28
7.	SLO2 and SLO4 versus G, NTU = 10, $\bar{\lambda} = .005$	30

LIST OF TABLES

Number		Page
1.	Independence of SLO3 and SLO5 from G	23
2.	Results of SLO3 and SLO5 for $\bar{\lambda} = 0.0$	24
3.	Independence of SLO 5 from G for $\bar{\lambda} = .04$	25
4.	Results of SLO2 and SLO4 for $\bar{\lambda} = 0.0$	26
5.	Results of SLO2 and SLO4 for $\bar{\lambda} = 0.005$	29

THE HISTORY OF THE

REIGN OF

CHARLES THE FIRST

BY

JOHN BURNET

OF

THE UNIVERSITY OF OXFORD

IN TWO VOLUMES.

THE FIRST

OF

THE REIGN

OF

CHARLES THE FIRST

BY

JOHN BURNET

NOMENCLATURE

A	total heat transfer area, ft^2 .
A_s	matrix cross sectional area, ft^2 .
C	step increase in fluid temperature, $= v_1 - v_0$, °F.
c_f	specific heat of fluid, BTU/lb °F.
c_s	specific heat of solid, BTU/lb °F.
h	heat transfer coefficient, BTU/hr ft^2 °F.
K_s	thermal conductivity of matrix, BTU/hr ft °F.
ℓ	total length of fluid flow path, ft.
λ	dimensionless conduction parameter, $= K_s A_s / w_f c_f$.
NTU	dimensionless heat transfer units, $= hA / w_f c_f$.
t	dimensionless time variable, $= hA\Theta / W_s c_s$.
Θ	time, hr.
u	solid temperature, °F.
u_0	reference solid temperature, °F.
v	fluid temperature, °F.
v_1	fluid temperature at $X = 0$, $t = 0 +$; °F.
v_0	reference fluid temperature, °F.
w_f	fluid mass flow rate, lb/hr.
W_s	mass of matrix, lb.
X	distance along the fluid flow path, ft.
x	dimensionless position variable, $= X / \ell$.

Table of Contents

1. Introduction	1
2. Theoretical Framework	2
3. Methodology	3
4. Data Collection	4
5. Results	5
6. Discussion	6
7. Conclusion	7
8. References	8
9. Appendix	9
10. Glossary	10
11. Bibliography	11
12. Index	12
13. Acknowledgments	13
14. About the Author	14
15. Contact Information	15
16. Disclaimer	16
17. Copyright	17
18. Privacy Policy	18
19. Terms of Service	19
20. Feedback	20
21. Updates	21
22. Support	22
23. Legal	23
24. Privacy	24
25. Security	25
26. Compliance	26
27. Accessibility	27
28. Sustainability	28
29. Diversity	29
30. Ethics	30
31. Governance	31
32. Risk Management	32
33. Quality Management	33
34. Environmental Management	34
35. Social Management	35
36. Human Resources Management	36
37. Financial Management	37
38. Information Management	38
39. Project Management	39
40. Change Management	40
41. Innovation Management	41
42. Performance Management	42
43. Risk Assessment	43
44. Risk Mitigation	44
45. Risk Monitoring	45
46. Risk Reporting	46
47. Risk Communication	47
48. Risk Culture	48
49. Risk Awareness	49
50. Risk Training	50
51. Risk Exercises	51
52. Risk Scenarios	52
53. Risk Indicators	53
54. Risk Metrics	54
55. Risk Benchmarks	55
56. Risk Targets	56
57. Risk Objectives	57
58. Risk Strategies	58
59. Risk Policies	59
60. Risk Procedures	60
61. Risk Guidelines	61
62. Risk Standards	62
63. Risk Codes of Practice	63
64. Risk Best Practices	64
65. Risk Lessons Learned	65
66. Risk Case Studies	66
67. Risk Examples	67
68. Risk References	68
69. Risk Further Reading	69
70. Risk Resources	70
71. Risk Tools	71
72. Risk Software	72
73. Risk Services	73
74. Risk Consultants	74
75. Risk Experts	75
76. Risk Professionals	76
77. Risk Organizations	77
78. Risk Associations	78
79. Risk Committees	79
80. Risk Groups	80
81. Risk Networks	81
82. Risk Communities	82
83. Risk Forums	83
84. Risk Conferences	84
85. Risk Seminars	85
86. Risk Workshops	86
87. Risk Webinars	87
88. Risk Podcasts	88
89. Risk Blogs	89
90. Risk Websites	90
91. Risk YouTube Channels	91
92. Risk Twitter Accounts	92
93. Risk LinkedIn Groups	93
94. Risk Facebook Pages	94
95. Risk Instagram Profiles	95
96. Risk Snapchat Accounts	96
97. Risk TikTok Accounts	97
98. Risk Twitch Channels	98
99. Risk YouTube Live Streams	99
100. Risk Podcast Episodes	100
101. Risk Blog Posts	101
102. Risk Website Articles	102
103. Risk YouTube Videos	103
104. Risk Twitter Tweets	104
105. Risk LinkedIn Posts	105
106. Risk Facebook Posts	106
107. Risk Instagram Posts	107
108. Risk Snapchat Snaps	108
109. Risk TikTok Videos	109
110. Risk Twitch Streams	110
111. Risk YouTube Live Streams	111
112. Risk Podcast Episodes	112
113. Risk Blog Posts	113
114. Risk Website Articles	114
115. Risk YouTube Videos	115
116. Risk Twitter Tweets	116
117. Risk LinkedIn Posts	117
118. Risk Facebook Posts	118
119. Risk Instagram Posts	119
120. Risk Snapchat Snaps	120
121. Risk TikTok Videos	121
122. Risk Twitch Streams	122
123. Risk YouTube Live Streams	123
124. Risk Podcast Episodes	124
125. Risk Blog Posts	125
126. Risk Website Articles	126
127. Risk YouTube Videos	127
128. Risk Twitter Tweets	128
129. Risk LinkedIn Posts	129
130. Risk Facebook Posts	130
131. Risk Instagram Posts	131
132. Risk Snapchat Snaps	132
133. Risk TikTok Videos	133
134. Risk Twitch Streams	134
135. Risk YouTube Live Streams	135
136. Risk Podcast Episodes	136
137. Risk Blog Posts	137
138. Risk Website Articles	138
139. Risk YouTube Videos	139
140. Risk Twitter Tweets	140
141. Risk LinkedIn Posts	141
142. Risk Facebook Posts	142
143. Risk Instagram Posts	143
144. Risk Snapchat Snaps	144
145. Risk TikTok Videos	145
146. Risk Twitch Streams	146
147. Risk YouTube Live Streams	147
148. Risk Podcast Episodes	148
149. Risk Blog Posts	149
150. Risk Website Articles	150
151. Risk YouTube Videos	151
152. Risk Twitter Tweets	152
153. Risk LinkedIn Posts	153
154. Risk Facebook Posts	154
155. Risk Instagram Posts	155
156. Risk Snapchat Snaps	156
157. Risk TikTok Videos	157
158. Risk Twitch Streams	158
159. Risk YouTube Live Streams	159
160. Risk Podcast Episodes	160
161. Risk Blog Posts	161
162. Risk Website Articles	162
163. Risk YouTube Videos	163
164. Risk Twitter Tweets	164
165. Risk LinkedIn Posts	165
166. Risk Facebook Posts	166
167. Risk Instagram Posts	167
168. Risk Snapchat Snaps	168
169. Risk TikTok Videos	169
170. Risk Twitch Streams	170
171. Risk YouTube Live Streams	171
172. Risk Podcast Episodes	172
173. Risk Blog Posts	173
174. Risk Website Articles	174
175. Risk YouTube Videos	175
176. Risk Twitter Tweets	176
177. Risk LinkedIn Posts	177
178. Risk Facebook Posts	178
179. Risk Instagram Posts	179
180. Risk Snapchat Snaps	180
181. Risk TikTok Videos	181
182. Risk Twitch Streams	182
183. Risk YouTube Live Streams	183
184. Risk Podcast Episodes	184
185. Risk Blog Posts	185
186. Risk Website Articles	186
187. Risk YouTube Videos	187
188. Risk Twitter Tweets	188
189. Risk LinkedIn Posts	189
190. Risk Facebook Posts	190
191. Risk Instagram Posts	191
192. Risk Snapchat Snaps	192
193. Risk TikTok Videos	193
194. Risk Twitch Streams	194
195. Risk YouTube Live Streams	195
196. Risk Podcast Episodes	196
197. Risk Blog Posts	197
198. Risk Website Articles	198
199. Risk YouTube Videos	199
200. Risk Twitter Tweets	200
201. Risk LinkedIn Posts	201
202. Risk Facebook Posts	202
203. Risk Instagram Posts	203
204. Risk Snapchat Snaps	204
205. Risk TikTok Videos	205
206. Risk Twitch Streams	206
207. Risk YouTube Live Streams	207
208. Risk Podcast Episodes	208
209. Risk Blog Posts	209
210. Risk Website Articles	210
211. Risk YouTube Videos	211
212. Risk Twitter Tweets	212
213. Risk LinkedIn Posts	213
214. Risk Facebook Posts	214
215. Risk Instagram Posts	215
216. Risk Snapchat Snaps	216
217. Risk TikTok Videos	217
218. Risk Twitch Streams	218
219. Risk YouTube Live Streams	219
220. Risk Podcast Episodes	220
221. Risk Blog Posts	221
222. Risk Website Articles	222
223. Risk YouTube Videos	223
224. Risk Twitter Tweets	224
225. Risk LinkedIn Posts	225
226. Risk Facebook Posts	226
227. Risk Instagram Posts	227
228. Risk Snapchat Snaps	228
229. Risk TikTok Videos	229
230. Risk Twitch Streams	230
231. Risk YouTube Live Streams	231
232. Risk Podcast Episodes	232
233. Risk Blog Posts	233
234. Risk Website Articles	234
235. Risk YouTube Videos	235
236. Risk Twitter Tweets	236
237. Risk LinkedIn Posts	237
238. Risk Facebook Posts	238
239. Risk Instagram Posts	239
240. Risk Snapchat Snaps	240
241. Risk TikTok Videos	241
242. Risk Twitch Streams	242
243. Risk YouTube Live Streams	243
244. Risk Podcast Episodes	244
245. Risk Blog Posts	245
246. Risk Website Articles	246
247. Risk YouTube Videos	247
248. Risk Twitter Tweets	248
249. Risk LinkedIn Posts	249
250. Risk Facebook Posts	250
251. Risk Instagram Posts	251
252. Risk Snapchat Snaps	252
253. Risk TikTok Videos	253
254. Risk Twitch Streams	254
255. Risk YouTube Live Streams	255
256. Risk Podcast Episodes	256
257. Risk Blog Posts	257
258. Risk Website Articles	258
259. Risk YouTube Videos	259
260. Risk Twitter Tweets	260
261. Risk LinkedIn Posts	261
262. Risk Facebook Posts	262
263. Risk Instagram Posts	263
264. Risk Snapchat Snaps	264
265. Risk TikTok Videos	265
266. Risk Twitch Streams	266
267. Risk YouTube Live Streams	267
268. Risk Podcast Episodes	268
269. Risk Blog Posts	269
270. Risk Website Articles	270
271. Risk YouTube Videos	271
272. Risk Twitter Tweets	272
273. Risk LinkedIn Posts	273
274. Risk Facebook Posts	274
275. Risk Instagram Posts	275
276. Risk Snapchat Snaps	276
277. Risk TikTok Videos	277
278. Risk Twitch Streams	278
279. Risk YouTube Live Streams	279
280. Risk Podcast Episodes	280
281. Risk Blog Posts	281
282. Risk Website Articles	282
283. Risk YouTube Videos	283
284. Risk Twitter Tweets	284
285. Risk LinkedIn Posts	285
286. Risk Facebook Posts	286
287. Risk Instagram Posts	287
288. Risk Snapchat Snaps	288
289. Risk TikTok Videos	289
290. Risk Twitch Streams	290
291. Risk YouTube Live Streams	291
292. Risk Podcast Episodes	292
293. Risk Blog Posts	293
294. Risk Website Articles	294
295. Risk YouTube Videos	295
296. Risk Twitter Tweets	296
297. Risk LinkedIn Posts	297
298. Risk Facebook Posts	298
299. Risk Instagram Posts	299
300. Risk Snapchat Snaps	300
301. Risk TikTok Videos	301
302. Risk Twitch Streams	302
303. Risk YouTube Live Streams	303
304. Risk Podcast Episodes	304
305. Risk Blog Posts	305
306. Risk Website Articles	306
307. Risk YouTube Videos	307
308. Risk Twitter Tweets	308
309. Risk LinkedIn Posts	309
310. Risk Facebook Posts	310
311. Risk Instagram Posts	311
312. Risk Snapchat Snaps	312
313. Risk TikTok Videos	313
314. Risk Twitch Streams	314
315. Risk YouTube Live Streams	315
316. Risk Podcast Episodes	316
317. Risk Blog Posts	317
318. Risk Website Articles	318
319. Risk YouTube Videos	319
320. Risk Twitter Tweets	320
321. Risk LinkedIn Posts	321
322. Risk Facebook Posts	322
323. Risk Instagram Posts	323
324. Risk Snapchat Snaps	324
325. Risk TikTok Videos	325
326. Risk Twitch Streams	326
327. Risk YouTube Live Streams	327
328. Risk Podcast Episodes	328
329. Risk Blog Posts	329
330. Risk Website Articles	330
331. Risk YouTube Videos	331
332. Risk Twitter Tweets	332
333. Risk LinkedIn Posts	333
334. Risk Facebook Posts	334
335. Risk Instagram Posts	335
336. Risk Snapchat Snaps	336
337. Risk TikTok Videos	337
338. Risk Twitch Streams	338
339. Risk YouTube Live Streams	339
340. Risk Podcast Episodes	340
341. Risk Blog Posts	341
342. Risk Website Articles	342
343. Risk YouTube Videos	343
344. Risk Twitter Tweets	344
345. Risk LinkedIn Posts	345
346. Risk Facebook Posts	346
347. Risk Instagram Posts	347
348. Risk Snapchat Snaps	348
349. Risk TikTok Videos	349
350. Risk Twitch Streams	350
351. Risk YouTube Live Streams	351
352. Risk Podcast Episodes	352
353. Risk Blog Posts	353
354. Risk Website Articles	354
355. Risk YouTube Videos	355
356. Risk Twitter Tweets	356
357. Risk LinkedIn Posts	357
358. Risk Facebook Posts	358
359. Risk Instagram Posts	359
360. Risk Snapchat Snaps	360
361. Risk TikTok Videos	361
362. Risk Twitch Streams	362
363. Risk YouTube Live Streams	363
364. Risk Podcast Episodes	364
365. Risk Blog Posts	365
366. Risk Website Articles	366
367. Risk YouTube Videos	367
368. Risk Twitter Tweets	368
369. Risk LinkedIn Posts	369
370. Risk Facebook Posts	370
371. Risk Instagram Posts	371
372. Risk Snapchat Snaps	372
373. Risk TikTok Videos	373
374. Risk Twitch Streams	374
375. Risk YouTube Live Streams	375
376. Risk Podcast Episodes	376
377. Risk Blog Posts	377
378. Risk Website Articles	378
379. Risk YouTube Videos	379
380. Risk Twitter Tweets	380
381. Risk LinkedIn Posts	381
382. Risk Facebook Posts	382
383. Risk Instagram Posts	383
384. Risk Snapchat Snaps	384
385. Risk TikTok Videos	385
386. Risk Twitch Streams	386
387. Risk YouTube Live Streams	387
388. Risk Podcast Episodes	388
389. Risk Blog Posts	389
390. Risk Website Articles	390
391. Risk YouTube Videos	391
392. Risk Twitter Tweets	392
393. Risk LinkedIn Posts	393
394. Risk Facebook Posts	394
395. Risk Instagram Posts	395
396. Risk Snapchat Snaps	396
397. Risk TikTok Videos	397
398. Risk Twitch Streams	398
399. Risk YouTube Live Streams	399
400. Risk Podcast Episodes	400
401. Risk Blog Posts	401
402. Risk Website Articles	402
403. Risk YouTube Videos	403
404. Risk Twitter Tweets	404
405. Risk LinkedIn Posts	405
406. Risk Facebook Posts	406
407. Risk Instagram Posts	407
408. Risk Snapchat Snaps	408
409. Risk TikTok Videos	409
410. Risk Twitch Streams	410
411. Risk YouTube Live Streams	411
412. Risk Podcast Episodes	412
413. Risk Blog Posts	413
414. Risk Website Articles	414
415. Risk YouTube Videos	415
416. Risk Twitter Tweets	416
417. Risk LinkedIn Posts	417
418. Risk Facebook Posts	418
419. Risk Instagram Posts	419
420. Risk Snapchat Snaps	420
421. Risk TikTok Videos	421
422. Risk Twitch Streams	422
423. Risk YouTube Live Streams	423
424. Risk Podcast Episodes	424
425. Risk Blog Posts	425
426. Risk Website Articles	426
427. Risk YouTube Videos	427
428. Risk Twitter Tweets	428
429. Risk LinkedIn Posts	429
430. Risk Facebook Posts	430
431. Risk Instagram Posts	431
432. Risk Snapchat Snaps	432
433. Risk TikTok Videos	433
434. Risk Twitch Streams	434
435. Risk YouTube Live Streams	435
436. Risk Podcast Episodes	436
437. Risk Blog Posts	437
438. Risk Website Articles	438
439. Risk YouTube Videos	439
440. Risk Twitter Tweets	440
441. Risk LinkedIn Posts	441
442. Risk Facebook Posts	442
443. Risk Instagram Posts	443
444. Risk Snapchat Snaps	444
445. Risk TikTok Videos	445
446. Risk Twitch Streams	446
447. Risk YouTube Live Streams	447
448. Risk Podcast Episodes	448
449. Risk Blog Posts	449
450. Risk Website Articles	450
451. Risk YouTube Videos	451
452. Risk Twitter Tweets	452
453. Risk LinkedIn Posts	453
454. Risk Facebook Posts	454
455. Risk Instagram Posts	455
456. Risk Snapchat Snaps	456
457. Risk TikTok Videos	457
458. Risk Twitch Streams	458
459. Risk YouTube Live Streams	459
460. Risk Podcast Episodes	460
461. Risk Blog Posts	461
462. Risk Website Articles	462
463. Risk YouTube Videos	463
464. Risk Twitter Tweets	464
465. Risk LinkedIn Posts	465
466. Risk Facebook Posts	466
467. Risk Instagram Posts	467
468. Risk Snapchat Snaps	468
469. Risk TikTok Videos	469
470. Risk Twitch Streams	470
471. Risk YouTube Live Streams	471
472. Risk Podcast Episodes	472
473. Risk Blog Posts	473
474. Risk Website Articles	474
475. Risk YouTube Videos	475
476. Risk Twitter Tweets	476
477. Risk LinkedIn Posts	477
478. Risk Facebook Posts	478
479. Risk Instagram Posts	479
480. Risk Snapchat Snaps	480
481. Risk TikTok Videos	481
482. Risk Twitch Streams	482
483. Risk YouTube Live Streams	483
484. Risk Podcast Episodes	484
485. Risk Blog Posts	485
486. Risk Website Articles	486
487. Risk YouTube Videos	487
488. Risk Twitter Tweets	488
489. Risk LinkedIn Posts	489
490. Risk Facebook Posts	490
491. Risk Instagram Posts	491
492. Risk Snapchat Snaps	492
493. Risk TikTok Videos	493
494. Risk Twitch Streams	494
495. Risk YouTube Live Streams	495
496. Risk Podcast Episodes	496
497. Risk Blog Posts	497
498. Risk Website Articles	498
499. Risk YouTube Videos	499
500. Risk Twitter Tweets	500
501. Risk LinkedIn Posts	501
502. Risk Facebook Posts	502
503. Risk Instagram Posts	503
504. Risk Snapchat Snaps	504
505. Risk TikTok Videos	505
506. Risk Twitch Streams	506
507. Risk YouTube Live Streams	507
508. Risk Podcast Episodes	508
509. Risk Blog Posts	509
510. Risk Website Articles	510
511. Risk YouTube Videos	511
512. Risk Twitter Tweets	512
513. Risk LinkedIn Posts	513
514. Risk Facebook Posts	514
515. Risk Instagram Posts	515
516. Risk Snapchat Snaps	516
517. Risk TikTok Videos	517
518. Risk Twitch Streams	518
519. Risk YouTube Live Streams	519
520. Risk Podcast Episodes	520
521. Risk Blog Posts	521
522. Risk Website Articles	522
523. Risk YouTube Videos	523

1. Introduction.

The "single blow" problem refers to the study of the transient heat transfer behavior of compact heat exchanger surfaces for the purpose of determining their heat transfer characteristics. Interest in compact heat exchangers has grown with the development of gas turbine engines. A regenerative cycle is desirable to increase the efficiency of the gas turbine. Proper design of a compact heat exchanger requires knowledge of the heat transfer characteristics of the various materials in numerous geometric configurations. Until recently it has been necessary to design and build the complete heat exchanger in order to determine its heat transfer characteristics experimentally. The objectives of the single blow studies are to determine the heat transfer characteristics from small test sections of the various matrices and to obtain considerable reduction in experimental costs.

The aim of the experimental testing is to obtain the exit fluid time-temperature history subsequent to a step change in the entrance fluid temperature. The experimental history must be compared to a theoretical time-temperature history to determine NTU, the dimensionless heat transfer parameter. The heat transfer coefficient, h , or the Colburn J factor can then be calculated.

In 1950 Locke [9] outlined five experimental techniques.¹ One of the simpler of these has become known as the "maximum slope" method. This technique compares the maximum slope of the experimental time-temperature history to the theoretical maximum slopes for various values of NTU and of λ , the longitudinal conduction parameter. With a cursory inspection, one might not appreciate the efficiency of this single point curve matching

¹Numbers in square brackets refer to the bibliography.

technique. One maximum slope represents a complete theoretical or a complete experimental curve. Therefore, it is unnecessary to calculate and plot vast quantities of theoretical time-temperature histories. This method eliminates the laborious and inaccurate matching of theoretical and experimental time-temperature histories, previously required to determine NTU. However, the maximum slope technique has two major limitations. The first problem is the difficulty in analytically solving the system of governing differential equations when longitudinal conductivities other than zero or infinity are included. The second problem is the magnification of experimental error due to curve matching. This problem is discussed in detail later.

Considerable analytical effort has been made to solve various aspects of the single blow problem since 1927 when Nusselt first studied it. Schumann [14] developed a solution in 1929 for zero conductivity in the direction of flow. His results are for a porous medium such as gravel but have been extended to include matrices consisting of metal balls, wire screens, or continuous materials for which the effects of longitudinal thermal conduction can be ignored. However, as indicated by Mondt [11] and Creswick [3], usually when the matrix is constructed of a continuous material in the flow direction, the effects of longitudinal conduction must be considered. Creswick outlined a finite difference technique to include this effect but his work was not complete enough to cover the area encountered in experimental testing. Mondt [11] obtained a closed solution for the limiting case of $\lambda = \infty$. Figure 1 indicates how drastically these two cases differ and shows the need for intermediate curves.



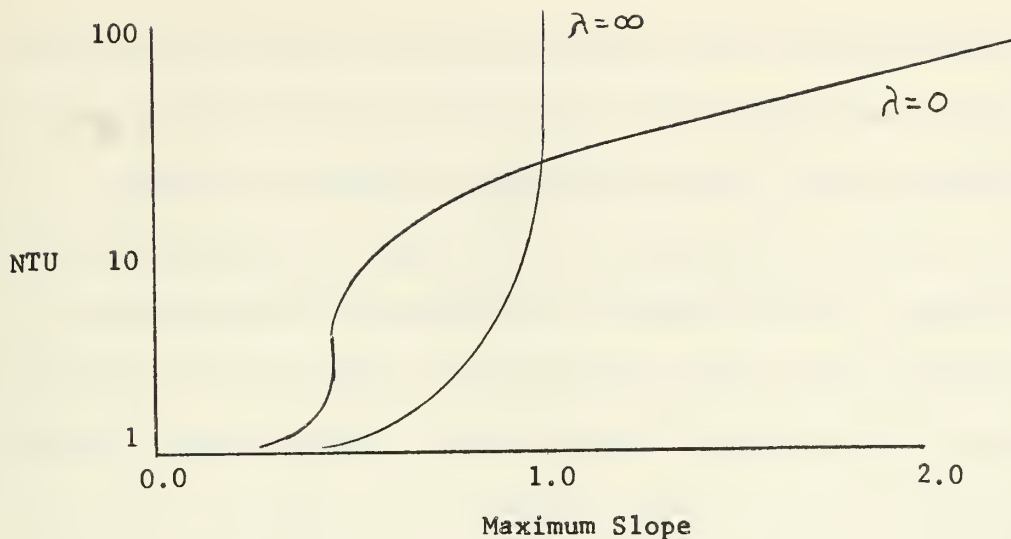


Figure 1

In 1948, F. E. Romie, et. al. [12] developed a system of partial differential equations governing the transient heat transfer behavior for hollow circular cylinders. Creswick arrived at the same set of equations for parallel plates. By a finite difference technique, he numerically approximated the solution of the system. However, difficulty with convergence was sometimes encountered. In 1963, C. P. Howard [5], guided by physical considerations, developed an alternate form of the finite-difference equations, and he was able to determine the convergence criteria and avoid the problem encountered by Creswick. Howard presented a table of results and a set of curves of NTU versus Maximum Slope for various values of λ . The table covers a range quite adequate for most experimental testing. As the values of NTU increased beyond 60, it became very difficult to obtain solutions with the finite difference technique due to the large computation times involved.

The objective of the solution presented in this paper is to verify or improve the results obtained by C. P. Howard and to avoid large computation times as NTU increases. This solution not only avoids the difficulty at

large values of NTU, but becomes faster as NTU increases due to the corresponding increase in the time at which the maximum slope occurs.

Referring to the error magnification due to curve matching, C. P. Howard [5] showed in Figure 3-A of his Appendix 3, that the error due to the experimental determination of maximum slope is magnified by a factor of two or greater when the value of NTU is determined by the maximum slope technique. The error magnification factor is defined as the ratio of percent error in NTU to percent error in experimental Maximum Slope. The essential features of the error factor as a function of NTU are indicated in Figure 2.

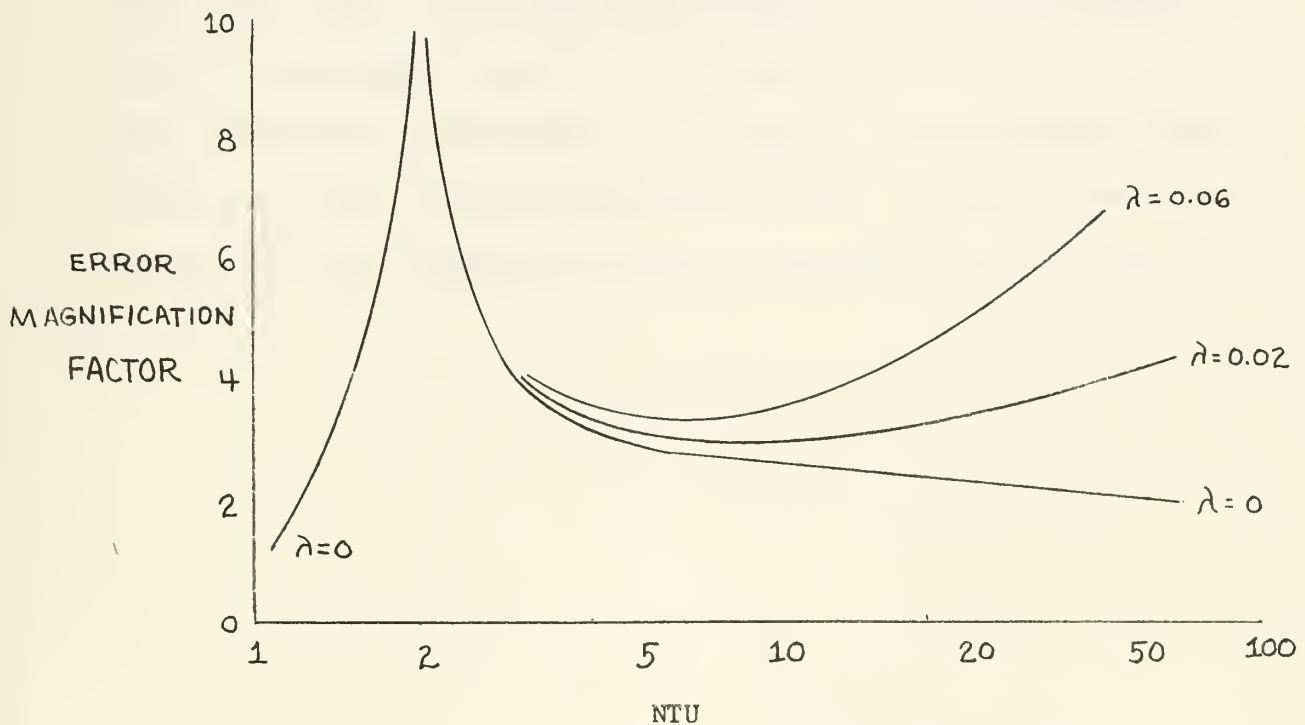


Figure 2

This figure shows that for the special case, $\lambda = 0$, the lowest error magnification is between 2.5 and 2 for NTU greater than five. At NTU near two there is a peak for which an accurate determination of NTU by maximum slope matching is impossible. When λ is non-zero, the peak

shifts to slightly higher values of NTU and the useful range above NTU of four decreases as $\bar{\lambda}$ increases. For example, for $\bar{\lambda} = .06$, an error factor of 3, at NTU = 5, is doubled at NTU = 28. Therefore, with this technique, one is forced to accept much larger errors as NTU and

$\bar{\lambda}$ increase. To avoid the inherent magnification of error, a modification can be made to the time-temperature curve matching technique with the aid of modern computers. When $\bar{\lambda}$ is finite, non-zero it is mandatory to use a computer to calculate the theoretical values of fluid temperature, given NTU, and t^2 . It would be elementary to include a least square error curve matching technique in the temperature program. Then, given three or more experimental values of fluid temperature and their corresponding values of t , the computer would compare the calculated theoretical temperatures at the given t 's for various NTU's and determine the NTU with the least square error. The anticipated error in any particular theoretical value of temperature is $\pm 1\%$ or less.

²"t" denotes the dimensionless time parameter.

2. Mathematical Technique.

The approach to be presented solved the system of partial differential equations for finite, non-zero \mathcal{A} by eliminating the variable of solid temperature. The result is a third order partial differential equation of fluid temperature as a function of time and x (the ratio of distance along the matrix to the total length). This equation and the necessary boundary conditions were transformed with respect to time by Laplace transformations to obtain a third order total differential equation with respect to x with parameter s . The equation was then solved for the transformed fluid temperature. The transformed boundary conditions were applied to determine the three arbitrary coefficients which were functions of the parameter s . Because the transformed solution was very complicated, numerical inversion was used to compute the inverse Laplace transform.

A Gaussian quadrature method, developed by H. Hurwitz, Jr. and P. F. Zweifel [6] for Fourier Transform Integrals, was adapted by L. A. Schmitt-roth [13] for the numerical inversion of Laplace Transforms. This technique avoids the difficulty encountered with alternating, slowly converging functions and proved to be essential for the successful inversion of this solution. For the two limiting cases $\mathcal{A} = 0$ and $\mathcal{A} = \infty$, a direct inversion of the Laplace solution was available.

REIGN OF KING CHARLES THE FIRST

IN THE YEAR OF HIS MAJESTY'S REIGN, 1649.

BY JOHN BURNET, BISHOP OF SALISBURY.

IN TWO VOLUMES.

LONDON, Printed by J. Streater, at the Sign of the Gun, in St. Dunstons Church-yard, 1680.

IN TWO VOLUMES.

THE SECOND VOLUME.

IN TWO VOLUMES.

THE SECOND VOLUME.

THE SECOND VOLUME.

THE SECOND VOLUME.

THE SECOND VOLUME.

THE SECOND VOLUME.

THE SECOND VOLUME.

THE SECOND VOLUME.

THE SECOND VOLUME.

THE SECOND VOLUME.

THE SECOND VOLUME.

THE SECOND VOLUME.

THE SECOND VOLUME.

3. Solution.

The governing differential equations for the transient heat transfer behavior including a finite, non-negative, longitudinal conductivity are as follows:³

$$(1) \quad \frac{\partial u}{\partial t} = (v - u) + \frac{\lambda}{NTU} \frac{\partial^2 u}{\partial x^2}$$

$$(2) \quad \frac{\partial v}{\partial x} = NTU (u - v)$$

The applicable boundary conditions are the following:

$$\begin{array}{ll} \text{a. } v(x, 0) = 0 & \text{d. } \frac{\partial u}{\partial x}(0, t) = 0 \\ \text{b. } \frac{\partial v}{\partial x}(x, 0) = 0 & \text{e. } \frac{\partial u}{\partial x}(1, t) = 0 \\ \text{c. } v(0, t) = C & \end{array}$$

The following is the approach used to solve this set of equations for the fluid temperature, v , and the slope of fluid temperature, $\frac{\partial v}{\partial x}$, respectively. In a similar manner the solid temperature, u , and other desired values can be obtained.

Solving equation 2 for u results in

$$(2a) \quad u = \frac{1}{NTU} \frac{\partial v}{\partial x} + v$$

The partial derivative of u with respect to t and the second partial of u with respect to x are determined from 2a, and then substituted into equation 1 to give

$$(3) \quad 0 = \frac{\partial^3 v(x, t)}{\partial x^3} + NTU \frac{\partial^2 v(x, t)}{\partial x^2} - \frac{NTU}{\lambda} \frac{\partial v(x, t)}{\partial x} \\ - \frac{NTU^2}{\lambda} \frac{\partial v(x, t)}{\partial t} - \frac{NTU}{\lambda} \frac{\partial^2 v(x, t)}{\partial x \partial t}$$

³The equations were developed from a heat balance by Creswick [3].

THE UNIVERSITY OF CHICAGO
DIVISION OF THE PHYSICAL SCIENCES
DEPARTMENT OF CHEMISTRY
530 SOUTH EAST ASIAN AVENUE
CHICAGO, ILLINOIS 60607-7070
TEL: 773/936-5000 FAX: 773/936-5001

RECEIVED
JAN 10 1997
10 10 1997

TO THE DIRECTOR
OF THE DIVISION OF THE PHYSICAL SCIENCES
FROM THE DEPARTMENT OF CHEMISTRY
RE: [illegible]

[illegible text block]

[illegible text block]

[illegible text block]

Each term in equation 3 is transformed with respect to t by Laplace transformation along with the following boundary conditions:

a. $v(x,0) = 0$

b. $\frac{\partial \mathcal{N}}{\partial X}(x,0) = 0$

The necessary transforms are

c. $\mathcal{L}\left\{\frac{\partial^3 \mathcal{N}}{\partial X^3}\right\} = \frac{\partial^3 \mathcal{N}}{\partial X^3}(X,S)$

etc.,

d. $\mathcal{L}\left\{\frac{\partial \mathcal{N}(x,t)}{\partial t}\right\} = \int_0^\infty \frac{\partial \mathcal{N}}{\partial t} e^{-st} dt = \mathcal{N}(x,t)e^{-st} \Big|_0^\infty + \int_0^\infty S [\mathcal{N}(x,t)] e^{-st} dt$
 $= -\mathcal{N}(x,0) + S[\mathcal{N}(x,S)]$

e. $\mathcal{L}\left\{\frac{\partial^2 \mathcal{N}(x,t)}{\partial X \partial t}\right\} = -\frac{\partial \mathcal{N}}{\partial X}(x,0) + S \frac{\partial \mathcal{N}}{\partial X}(x,S)$

Substitution of these values in equation 3 after applying the above boundary conditions, results in

$$(3a). \quad 0 = \frac{\partial^3 \mathcal{N}(X,S)}{\partial X^3} + NTU \frac{\partial^2 \mathcal{N}(X,S)}{\partial X^2} - \frac{NTU(S+1)}{\lambda} \frac{\partial \mathcal{N}(X,S)}{\partial X} - \frac{NTU^2 S}{\lambda} \mathcal{N}(X,S).$$

The corresponding auxiliary equation is

$$(3b). \quad r^3 + NTU r^2 - \frac{NTU}{\lambda} (S+1) r - \frac{NTU^2}{\lambda} S = 0$$

The general solution in the Laplace s-plane for the fluid temperature is

$$(4). \quad \mathcal{N}(X,S) = C_1(S) e^{r_1 X} + C_2(S) e^{r_2 X} + C_3(S) e^{r_3 X}$$

where r_1, r_2, r_3 are the roots of equation (3b).

The boundary conditions c, d, and e are transformed and then used to determine the coefficients C_1, C_2 , and C_3 . The transform of c is

$$\mathcal{N}(0,S) = \frac{C}{S}.$$

The transform of d is $\frac{\partial u}{\partial x}(0,s) = 0$, and similarly for e,
 $\frac{\partial u}{\partial x}(1,s) = 0$.

From equation 2a the following equation is obtained:

$$(5). \quad \frac{\partial u}{\partial x}(x,t) = \frac{1}{NTU} \frac{\partial^2 w}{\partial x^2} + \frac{\partial w}{\partial x}(x,t).$$

Applying boundary condition c to equation 4 gives

$$(6). \quad w(0,s) = C_1(s) + C_2(s) + C_3(s) = \frac{C}{s}.$$

Rather than apply boundary conditions d and e directly it is convenient to use their equivalent form in terms of v. To apply boundary condition d it is necessary to transform equation 5 which results in

$$\frac{\partial u}{\partial x}(x,s) = \frac{1}{NTU} \frac{\partial^2 w}{\partial x^2}(x,s) + \frac{\partial w}{\partial x}(x,s) \quad \text{therefore;}$$

$$\frac{\partial u}{\partial x}(0,s) = \frac{1}{NTU} \frac{\partial^2 w}{\partial x^2}(0,s) + \frac{\partial w}{\partial x}(0,s) = 0.$$

When this boundary condition is applied the following equation is obtained:

$$(7). \quad \frac{1}{NTU} (\eta_1^2 C_1(s) + \eta_2^2 C_2(s) + \eta_3^2 C_3(s)) + \eta_1 C_1(s) + \eta_2 C_2(s) + \eta_3 C_3(s) = 0.$$

The application of boundary condition e is similar, resulting in

$$(8). \quad \frac{1}{NTU} (\eta_1^2 C_1 e^{\eta_1} + \eta_2^2 C_2 e^{\eta_2} + \eta_3^2 C_3 e^{\eta_3}) + \eta_1 C_1 e^{\eta_1} + \eta_2 C_2 e^{\eta_2} + \eta_3 C_3 e^{\eta_3} = 0.$$

(8a). Define $R_n \equiv \left(\frac{\eta_n^2}{NTU} + \eta_n \right)$ where $n = 1, 2, 3$. Then the following matrix equation can be set up using equations 6, 7, 8.

THE UNIVERSITY OF CHICAGO
LIBRARY

THE UNIVERSITY OF CHICAGO
LIBRARY

THE UNIVERSITY OF CHICAGO
LIBRARY

THE UNIVERSITY OF CHICAGO
LIBRARY

THE UNIVERSITY OF CHICAGO
LIBRARY

THE UNIVERSITY OF CHICAGO
LIBRARY

THE UNIVERSITY OF CHICAGO
LIBRARY

$$\begin{bmatrix} \frac{C}{s} \\ 0 \\ 0 \end{bmatrix} = \begin{bmatrix} 1 & 1 & 1 \\ R_1 & R_2 & R_3 \\ R_1 e^{n_1} & R_2 e^{n_2} & R_3 e^{n_3} \end{bmatrix} \cdot \begin{bmatrix} C_1(s) \\ C_2(s) \\ C_3(s) \end{bmatrix}$$

To solve for C_1 , C_2 , C_3 , Cramer's Rule is applied. The denominator is

$$\Delta = \left[R_2 R_3 (e^{n_3} - e^{n_2}) + R_1 R_3 (e^{n_1} - e^{n_3}) + R_1 R_2 (e^{n_2} - e^{n_1}) \right].$$

The three arbitrary coefficients are the following:

$$C_1(s) = \frac{\begin{vmatrix} C/s & 1 & 1 \\ 0 & R_2 & R_3 \\ 0 & R_2 e^{n_2} & R_3 e^{n_3} \end{vmatrix}}{\Delta} = \frac{\frac{C}{s} [R_2 R_3 e^{n_3} - R_2 R_3 e^{n_2}]}{\Delta},$$

$$C_2(s) = \frac{\begin{vmatrix} 1 & C/s & 1 \\ R_1 & 0 & R_3 \\ R_1 e^{n_1} & 0 & R_3 e^{n_3} \end{vmatrix}}{\Delta} = \frac{\frac{C}{s} [R_1 R_3 e^{n_1} - R_1 R_3 e^{n_3}]}{\Delta} \quad \text{and}$$

$$C_3(s) = \frac{\begin{vmatrix} 1 & 1 & C/s \\ R_1 & R_2 & 0 \\ R_1 e^{n_1} & R_2 e^{n_2} & 0 \end{vmatrix}}{\Delta} = \frac{\frac{C}{s} [R_1 R_2 e^{n_2} - R_1 R_2 e^{n_1}]}{\Delta}.$$

Substituting C_1 , C_2 , and C_3 into equation 4 results in

1871

1872

1873

1874

1875

1876

1877

1878

1879

$$v(x,s) = \frac{C}{s} \frac{[R_2 R_3 (e^{n_3} - e^{n_2}) e^{n_1 x} + R_1 R_3 (e^{n_1} - e^{n_3}) e^{n_2 x} + R_1 R_2 (e^{n_2} - e^{n_1}) e^{n_3 x}]}{\Delta} \quad (9)$$

Evaluating equation 9 at $x = 1$ results in the following:

$$v(1,s) = \frac{C}{s} \frac{\{R_2 R_3 [e^{(n_3+n_1)} - e^{(n_2+n_1)}] + R_1 R_3 [e^{(n_1+n_2)} - e^{(n_3+n_2)}] + R_1 R_2 [e^{(n_2+n_3)} - e^{(n_1+n_3)}]\}}{R_2 R_3 (e^{n_3} - e^{n_2}) + R_1 R_3 (e^{n_1} - e^{n_3}) + R_1 R_2 (e^{n_2} - e^{n_1})} \quad (10)$$

Recall that the Laplace operation $Sf(s) = F(+0)$ corresponds to

$\frac{d}{dt} F(t)$. It follows directly that $\frac{\partial v}{\partial t}(1,t)$ is equal to the operation $S \cdot v(1,s)$, since $v(1,0) = 0$ by boundary condition 2. Therefore,

$$(11) \quad \frac{\partial v}{\partial t}(1,s) = S \cdot v(1,s)$$

To determine the exit fluid temperature and the slope with respect to time of the exit fluid temperature, it is necessary to find the inverse Laplace transforms of equations 9 and 10 respectively. If the values of R_i and r_i , $i = 1, 2, 3$; were not functions of s this step would be elementary. Unfortunately, the values of R and r are indeed functions of s as indicated by equations 8a and 3b respectively. Therefore, for this particular case the task of finding an analytic inverse transform is nearly hopeless.

Rather than proceed further on this approach, a computer program to calculate the complex roots for given values of s , NTU, and \mathcal{R} , is used. Consequently, this step precludes any possibility of finding an analytical solution if one exists. Now, the value of $v(1,s)$ or $\frac{\partial v}{\partial t}$ at $(1,s)$ can be determined for any set of the parameters, C , s , NTU, and \mathcal{R} ,

THE UNIVERSITY OF CHICAGO
DEPARTMENT OF THE HISTORY OF ARTS
AND ARCHITECTURE

THE UNIVERSITY OF CHICAGO
DEPARTMENT OF THE HISTORY OF ARTS
AND ARCHITECTURE

THE UNIVERSITY OF CHICAGO
DEPARTMENT OF THE HISTORY OF ARTS
AND ARCHITECTURE

THE UNIVERSITY OF CHICAGO
DEPARTMENT OF THE HISTORY OF ARTS
AND ARCHITECTURE

THE UNIVERSITY OF CHICAGO
DEPARTMENT OF THE HISTORY OF ARTS
AND ARCHITECTURE

THE UNIVERSITY OF CHICAGO
DEPARTMENT OF THE HISTORY OF ARTS
AND ARCHITECTURE

THE UNIVERSITY OF CHICAGO
DEPARTMENT OF THE HISTORY OF ARTS
AND ARCHITECTURE

THE UNIVERSITY OF CHICAGO
DEPARTMENT OF THE HISTORY OF ARTS
AND ARCHITECTURE

and the Laplace inversion integral may be used to find $v(1,t)$. Finding an adequate numerical technique to evaluate this inversion integral was no simple matter.

When Simpson's Rule was applied to evaluate the inversion integral using the real (VR) and imaginary (VI) parts of $v(1,s)$, the results were grossly in error, the behavior being as described in reference [6] and [13]. The numerical technique described in reference [13] was found to be greatly superior to Simpson's Rule for this particular problem. It incorporates a technique to accelerate convergence of an alternating series, and uses Gauss-Chebyshev formulas for integration. This technique uses either the real part (VR) or the imaginary part (VI) and results in two different forms. Since there are no known values for this solution it was necessary to use both of these forms to be confident that the correct solutions were obtained.

According to the theory of Laplace inversion, the inversion integral,⁴

$$\frac{1}{2\pi i} \int_{G-i\infty}^{G+i\infty} v(x,s) e^{st} ds$$

, should be independent of G , where $s = G + iy$. When this approach was used with Simpson's Rule none of the results were independent of G . Recall the form of the inversion integral

$$\frac{e^{Gt}}{\pi} \int_0^{\infty} v(x,G,y) e^{iyt} dy$$

. Since the region initially investigated used $t = 7$ and G of .5, 1 and 2, any error in the numerical technique was greatly multiplied giving very poor results. However; this indicated that G is an additional parameter that must be determined for each new program. Rather than cause difficulty, this parameter proves to be essential. For the same G , it was found that one program gave consistently low results while the other was consistently high. Then by

⁴Churchill, op. cit., p. 176.

varying G of both programs the program using VR can be made to agree with the results of the program using VI. This is the approach that was used to make the various programs converge to a solution. The numerical technique outlined in [13] uses Chebyshev's polynomial to fit the function $f(s)$. It was found that this polynomial is very sensitive to a small change in G . For example, upon changing G from 0.0 to 0.05, the product (slope \cdot NTU) changed from 1.0877 to 1.1333 an increase of 4.19%. Again according to theory, results should be independent of G . Therefore, two new programs were written using a Gauss-Legendre quadrature format to integrate VR or VI. These programs were found to be essentially independent of G for reasonable increments of G . For example changing G from 0.0 to 0.06, the slope \cdot NTU changed from 1.10096 to 1.09776 a decrease of 0.29%. Figure 3 indicates a comparison of these two programs. On this basis alone, it is felt that the Legendre polynomial is more accurate. Unfortunately, in comparison to the programs using the Chebyshev polynomial it is considerably slower. Because of this fact, the Legendre programs which include an error analysis are being used to determine accurate test values for the determination of the best G for each program. Once the best G is determined, the speedier Chebyshev programs can be used for long data runs.

The integration technique described in detail in references [6] and [13] will be described here as it was applied to this problem. The inversion integral is the following:

$$(12) \quad \mathcal{L}^{-1}\{f(s)\} = f(t) = \frac{1}{2\pi i} \int_{G-i\infty}^{G+i\infty} f(s) e^{-st} ds$$

Then writing $f(s)$ as the sum of the real and imaginary parts results in

THE UNIVERSITY OF CHICAGO

PHILOSOPHY DEPARTMENT

1100 S. EAST ASIAN AVENUE, CHICAGO, ILL. 60607

TEL: (773) 936-5000 FAX: (773) 936-5001

WWW.PHIL.DEP.UCHICAGO.EDU

CHICAGO, ILL. 60607-7073

CHICAGO, ILL. 60607-7073

CHICAGO, ILL. 60607-7073

CHICAGO, ILL. 60607-7073

CHICAGO, ILL. 60607-7073

CHICAGO, ILL. 60607-7073

CHICAGO, ILL. 60607-7073

CHICAGO, ILL. 60607-7073

CHICAGO, ILL. 60607-7073

CHICAGO, ILL. 60607-7073

CHICAGO, ILL. 60607-7073

CHICAGO, ILL. 60607-7073

CHICAGO, ILL. 60607-7073

CHICAGO, ILL. 60607-7073

CHICAGO, ILL. 60607-7073

CHICAGO, ILL. 60607-7073

CHICAGO, ILL. 60607-7073

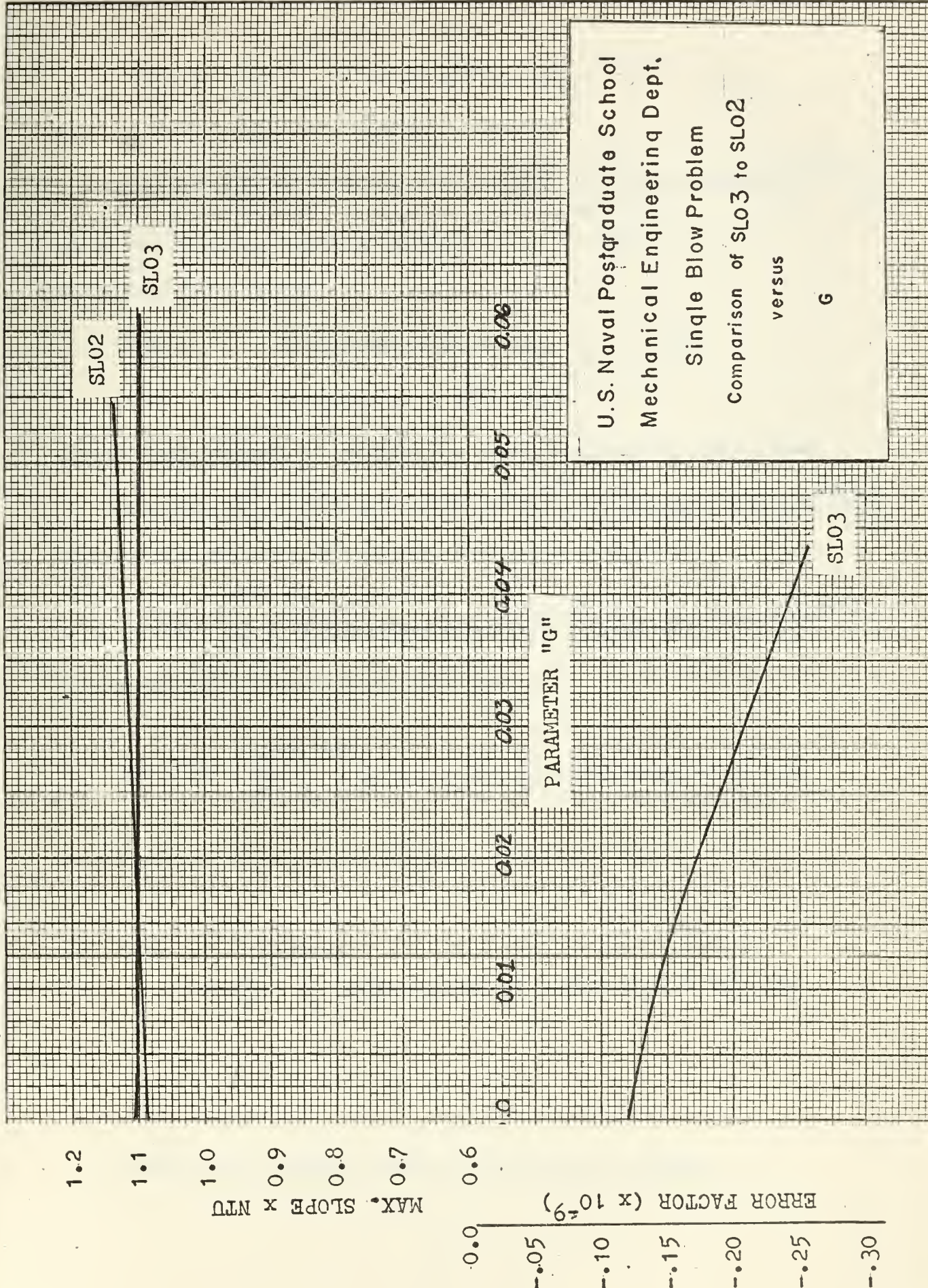
CHICAGO, ILL. 60607-7073

CHICAGO, ILL. 60607-7073

CHICAGO, ILL. 60607-7073

CHICAGO, ILL. 60607-7073

CHICAGO, ILL. 60607-7073



U.S. Naval Postgraduate School
 Mechanical Engineering Dept.
 Single Blow Problem
 Comparison of SL03 to SL02
 versus
 G

FIGURE 3



$$f(t) = \frac{1}{2\pi i} \int_{-\infty}^{\infty} [\phi(G+iy) + i\psi(G+iy)] e^{t(G+iy)} (idy).$$

The inversion integral can then be written as

$$(12a) \quad f(t) = \frac{e^{Gt}}{2\pi} \left\{ \int_{-\infty}^0 [\phi(G+iy) + i\psi(G+iy)] e^{iyt} dy + \int_0^{\infty} [\phi(G+iy) + i\psi(G+iy)] e^{iyt} dy \right\},$$

where the following condition applies: $f(\bar{s}) = \overline{f(s)}$.

It follows directly that

$$(12b) \quad \phi(G+iy) = \phi(G-iy) \quad , \quad \text{and}$$

$$(12c) \quad \psi(G+iy) = -\psi(G-iy).$$

In the first integral of equation 12a, let $y = -y'$, and $dy = -dy'$, then

$$(13) \quad f(t) = \frac{e^{Gt}}{2\pi} \left\{ \int_0^{\infty} [\phi(G-iy') + i\psi(G-iy')] e^{-iy't} dy' + \int_0^{\infty} [\phi(G+iy) + i\psi(G+iy)] e^{iyt} dy \right\}.$$

Applying the relations 12b and 12c, equation 13 reduces to

$$f(t) = \frac{e^{Gt}}{2\pi} \int_0^{\infty} \left\{ [\phi(G+iy) - i\psi(G+iy)] e^{-iyt} + [\phi(G+iy) + i\psi(G+iy)] e^{iyt} \right\} dy.$$

On rearranging and simplifying, this becomes

$$(14) \quad f(t) = \frac{e^{Gt}}{\pi} \int_0^{\infty} [\phi(G+iy) \cos yt - \psi(G+iy) \sin yt] dy.$$

By definition of the inverse integral, $f(-t) = 0$. Thus

$$(15) \quad 0 = \frac{e^{-Gt}}{\pi} \int_0^{\infty} [\phi(G+iy) \cos yt + \psi(G+iy) \sin yt] dy,$$

⁵ A bar over a quantity indicates the complex conjugate.



which reduces to

$$\int_0^{\infty} \phi(G+iy) \cos yt \, dy = -\int_0^{\infty} \psi(G+iy) \sin yt \, dy.$$

Two forms of $f(t)$ can be found by expressing the integrals either in terms of the real or the imaginary parts. They are respectively

$$(16) \quad f(t) = \frac{2e^{Gt}}{\pi} \int_0^{\infty} \phi(G+iy) \cos yt \, dy, \text{ and}$$

$$(17) \quad f(t) = -\frac{2e^{Gt}}{\pi} \int_0^{\infty} \psi(G+iy) \sin yt \, dy.$$

These two equations are the basis of the two programs mentioned earlier. In general discussions VR will represent the function $\phi \cos yt$ and VI the function $\psi \sin yt$. The Gaussian quadrature formula using either Chebyshev's or Legendre's polynomial is used to evaluate the integral from zero to infinity. Both functions VR and VI are of the general form shown in Figure 4

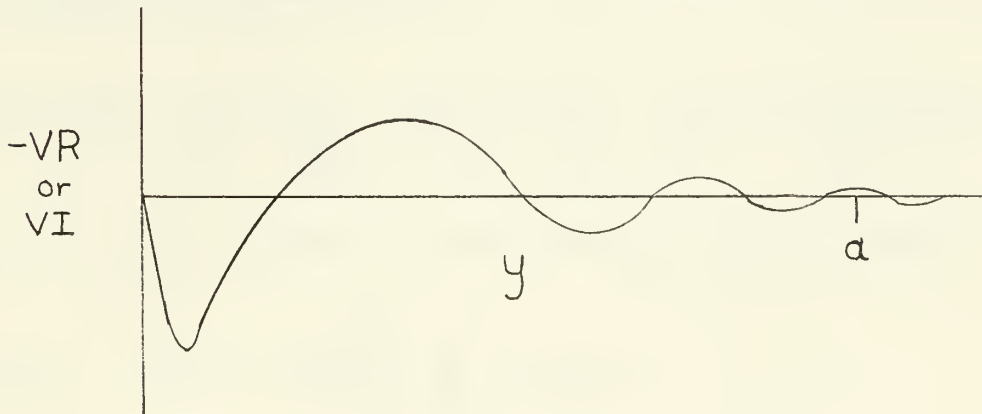


Figure 4

If the function were integrated with respect to y and the summation stopped at a , there would be significant error. Two operations are

THE
JOURNAL OF THE
ROYAL ANTHROPOLOGICAL INSTITUTE
OF GREAT BRITAIN AND IRELAND
VOLUME 34. PART 1. 1904.
LONDON: PUBLISHED BY THE INSTITUTE.
1904.

CONTENTS.
PAGES.
The Evolution of Man. By H. H. S. G. 1
The Evolution of Man. By H. H. S. G. 1
The Evolution of Man. By H. H. S. G. 1
The Evolution of Man. By H. H. S. G. 1
The Evolution of Man. By H. H. S. G. 1
The Evolution of Man. By H. H. S. G. 1
The Evolution of Man. By H. H. S. G. 1
The Evolution of Man. By H. H. S. G. 1
The Evolution of Man. By H. H. S. G. 1
The Evolution of Man. By H. H. S. G. 1

THE
JOURNAL OF THE
ROYAL ANTHROPOLOGICAL INSTITUTE
OF GREAT BRITAIN AND IRELAND
VOLUME 34. PART 2. 1904.
LONDON: PUBLISHED BY THE INSTITUTE.
1904.

included in this solution to reduce the error. The first operation is an averaging technique which accelerates convergence. The second operation involves integrating each half wave and then summing them. To accomplish this we introduce the following change of variable in Equation 17.

$$\text{Let } x = \frac{t}{\pi} y - \frac{1}{2} \quad \text{therefore } y = \frac{\pi}{t} (x + \frac{1}{2}) \quad \text{and } dy = \frac{\pi}{t} dx.$$

Applying these to equation 17 results in

$$\begin{aligned} (17a) \quad f(t) &= - \frac{2e^{Gt}}{t} \int_{-\frac{1}{2}}^{\infty} \mathcal{U} \left[G + i \frac{\pi}{t} (x + \frac{1}{2}) \right] \sin \pi (x + \frac{1}{2}) dx, \\ &= - \frac{2e^{Gt}}{t} \sum_{m=0}^{\infty} \int_{-\frac{1}{2}+m}^{\frac{1}{2}+m} \mathcal{U} \left[G + i \frac{\pi}{t} (x + \frac{1}{2}) \right] \sin \pi (x + \frac{1}{2}) dx. \end{aligned}$$

Now let $x' = x - m$, then

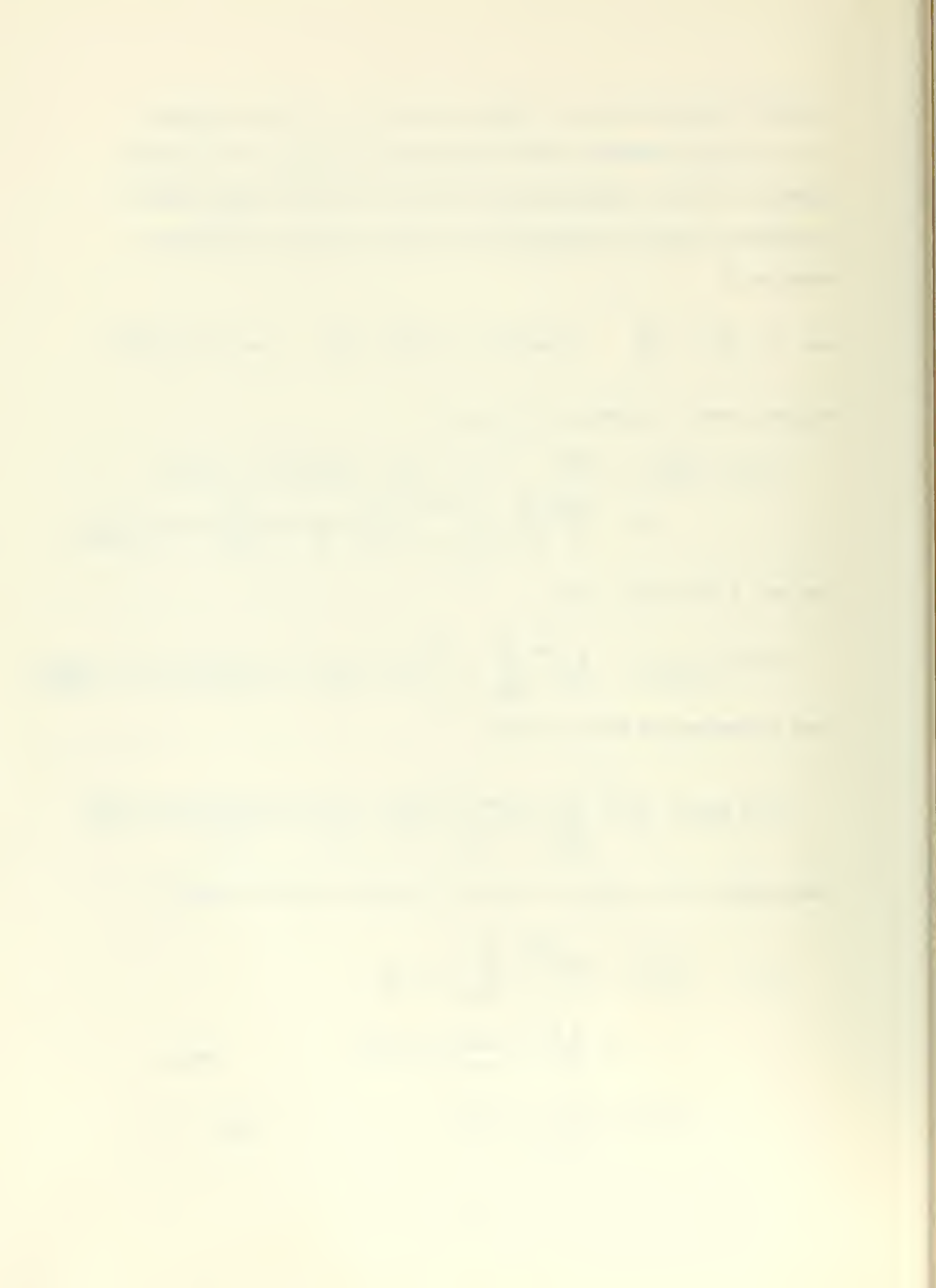
$$(17b) \quad f(t) = - \frac{2e^{Gt}}{t} \sum_{m=0}^{\infty} \int_{-\frac{1}{2}}^{\frac{1}{2}} \mathcal{U} \left[G + i \frac{\pi}{t} (x' + m + \frac{1}{2}) \right] \sin \pi (x' + m + \frac{1}{2}) dx'.$$

Upon suppressing the prime, we have

$$(18) \quad f(t) = \frac{2e^{Gt}}{t} \sum_{m=0}^{\infty} (-1)^{m+1} \int_{-\frac{1}{2}}^{\frac{1}{2}} \mathcal{U} \left[G + i \frac{\pi}{t} (x + m + \frac{1}{2}) \right] \cos \pi x dx$$

When equation 18 is written in terms of partial sums, the result is

$$\begin{aligned} (19) \quad f(t) &= \frac{2e^{Gt}}{t} \sum_{m=0}^{\infty} I_m(t) \\ &= \frac{2e^{Gt}}{t} \lim_{m \rightarrow \infty} S_m(t), \quad \text{where} \\ S_m(t) &= \sum_{m=0}^m I_m(t) \quad \text{and} \end{aligned}$$



$$(19a) \quad I_m(t) = (-1)^{m+1} \int_{-\frac{1}{2}}^{\frac{1}{2}} \psi \left[G + i \frac{\pi}{t} (x + m + \frac{1}{2}) \right] \cos(\pi x) dx.$$

Again referring to [13], L. A. Schmittroth applied a Gaussian quadrature method to evaluate $I_n(t)$. $I_n(t)$ can be approximated as follows:

$$(19b) \quad I_m(t) \approx (-1)^{m+1} \sum_{j=1}^N \frac{W_j^N}{\cos \pi y_j^N} \left[\psi(-\omega) + \psi(+\omega) \right]$$

where

$$(19c) \quad y_j^N = \frac{2j-1}{2(2N+1)}, \quad j = 1, 2, 3, \dots, N$$

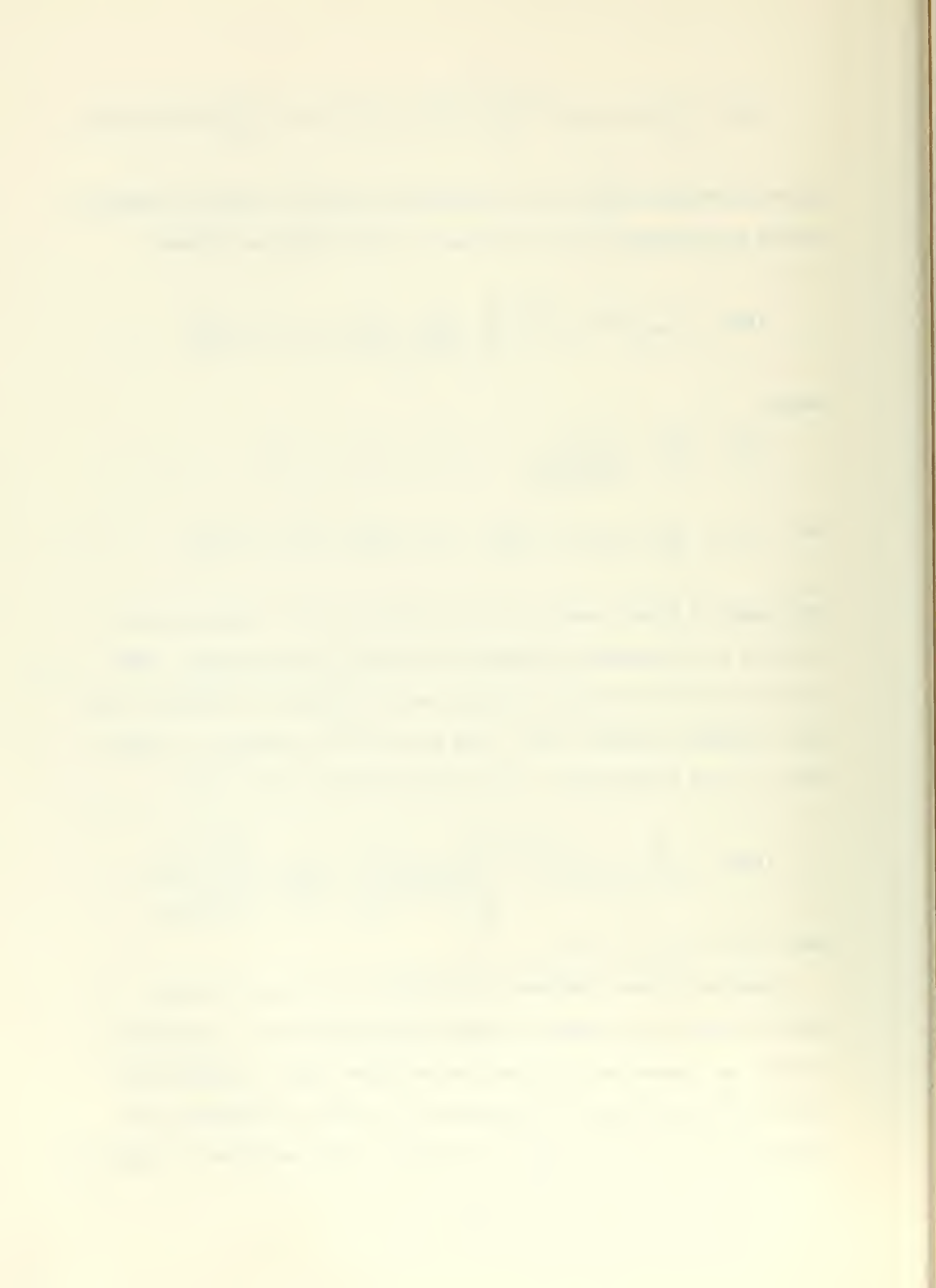
$$\text{and} \quad -\omega = \frac{\pi}{t} \left(-y_j^N + m + \frac{1}{2} \right); \quad +\omega = \frac{\pi}{t} \left(y_j^N + m + \frac{1}{2} \right).$$

The number of points used to fit the function is $2N$. Obviously, the larger N is, the greater the degree of accuracy one can expect. This is the core of the iterative process and an adequate N is desired to ensure reasonable computer time. This point will be discussed in detail later. The N coefficients W_j^N are the solutions of the system.

$$(19d) \quad 2 \sum_{j=1}^N W_j^N \cos^{2N-2} \left[\frac{(2j-1)\pi}{2(2N+1)} \right] = \frac{1}{\sqrt{\pi}} \frac{\Gamma(p+\frac{1}{2})}{\Gamma(p+1)},$$

where $p = 1, 2, \dots, N$.

Equation 19 uses Chebyshev's polynomial for the curve fitting. A similar form of $I_n(t)$ can be developed from Equation 16. As mentioned earlier, an integration technique was developed using a Legendre polynomial for curve fitting. If equation 16 is used to illustrate this approach, the relation $\lambda = \frac{ty}{\pi}$ is required. Then equation 16 reduces to:



$$(20) \quad f(t) = \frac{2e^{Gt}}{t} \int_0^{\infty} \phi(G + i\frac{\pi}{t}x) \cos \pi x dx.$$

Now, the Gaussian quadrature method can be applied as above. For the Gauss-Legendre formulas, a change of variable was applied to equation 17b to set up the infinite sum of integrals from zero to one, one to two and so on rather than a sum of integrals evaluated from -1/2 to 1/2.

The Gauss-Chebyshev and the Gauss-Legendre formulas applied to the real or imaginary form of the inversion integral produce four different computer programs. Any one of these should give the correct solution, but one form may prove to be better for a particular application.

For zero and infinite longitudinal conduction, the governing differential equations reduce to much simpler forms. The solutions for both cases are given in Appendix I and are in complete agreement with the solutions of Schumman and Mondt for $\bar{\alpha} = 0$ and $\bar{\alpha} = \infty$ respectively.

4. Computer Program.

The principal objective of the computer program is to solve for the maximum slope⁶ of fluid temperature at $X = \ell$. The main program is designed to determine the slope of the fluid temperature at $X = \ell$ which is the numerical inversion of equation 11.

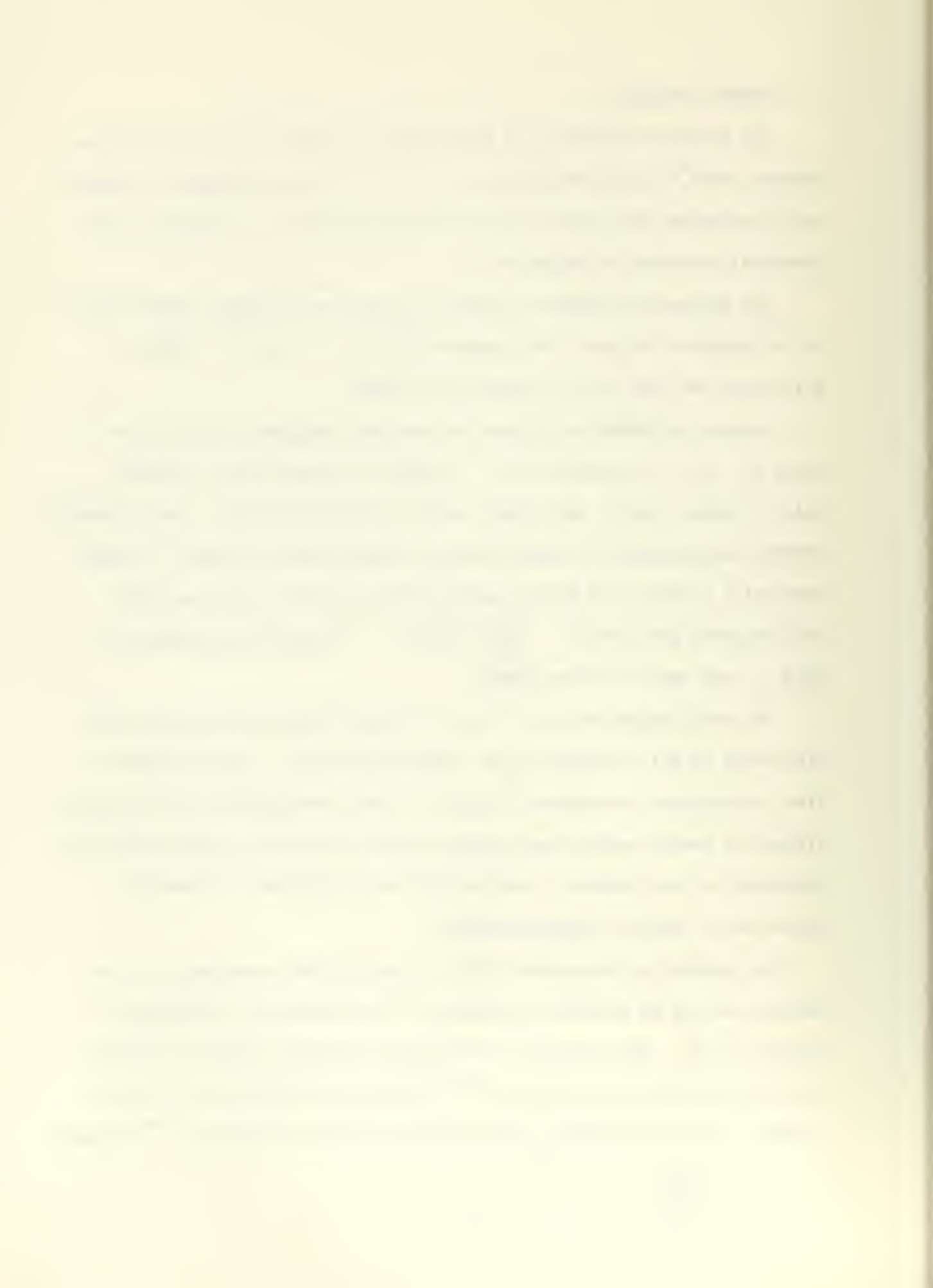
The subroutine SOOTS2 calculates the real and imaginary coefficients of the equation 3b given the parameters NTU, λ , G, and Y. These coefficients are then put into subroutine TOOTS2.

Subroutine TOOTS2 calculates the real and imaginary parts of the roots r_1, r_2, r_3 of equation 3b. It sends its results back to SOOTS2 which arranges them in the proper order and subscripts them appropriately. SOOTS2 then provides the proper roots as input values to EVAL. The EVAL subroutine provides the main program with the values of the real (VR) and imaginary part (VI) of $\frac{\partial n}{\partial t}(1, S)$, given the parameters G, $\frac{\pi X}{t}$, C, and the roots from SOOTS2.

The main program will call for N of these values (see equation 19c) with which it will calculate $I_0(t)$ (see equation 19). The programmer is free to determine the number of $I_n(t)$'s to sum, where $\sum_{n=0}^m I_n(t) = S_m(t)$. Fifteen to twenty partial sums appear to be sufficient for the function encountered in this problem. Each partial sum calculated is stored and serves as an input to subroutine AVER.

The purpose of subroutine AVER is to accelerate convergence of the partial sums by an averaging technique. This technique is discussed in reference [6]. The subroutine will take an arbitrary number of partial sums and calculate any specified n^{th} average, and return it to the main program. It also calculates the difference between successive n^{th} averages

$$^6 \text{i.e., } \frac{\partial n}{\partial t}.$$



returning it to the main program. The main program then requires this difference to be less than an arbitrarily specified value (EP). If the difference is larger than EP, the main program increases the number of partial sums by LD and calls AVER again until the difference is less than EP. At this point, the value of the accelerated partial sum is accepted and the slope is calculated. However, the slope calculated for a particular value of dimensionless time is not the value desired. It is necessary to search for the maximum slope by varying time.

Initially, a search using an incremental step of time was used. This was eventually abandoned because it would find relative maxima only and it was tediously slow if a poor choice were made for a starting time. It should be noted that theoretical relative maxima have been found for small values of NTU and negative slopes have also been noted. J. M. Bannon^[1] is concurrently conducting an experimental thesis and has experimentally found relative maxima and negative slopes for high mass flow or small values of NTU. It would be interesting to compare a theoretical time temperature curve for his experimental value of \hat{N} with his experimental time-temperature curve.

The purpose of SLOMAX is to find the maximum slope. To avoid the problem of choosing a poor starting time, a reasonable range of t is chosen. A rule of thumb is that the largest maximum slope will occur at a time less than or equal to NTU. SLOMAX uses a parabola curve fitting technique with three points.

The first and last of the three points are program input values of time and the middle point is the arithmetic mean. The slopes are calculated for the first two values of time and then tested to ensure that the

middle slope is larger than the first. This is necessary to obtain the maximum rather than a minimum slope. Then the third value of slope is calculated and tested to insure that it is less than the middle slope. The program has the ability to adjust the arbitrary values of time to ensure the middle slope is the largest. Once this basic shape is obtained the program calculates the value of time at which the parabola has a maximum. This process is repeated using the calculated maximum time and slope as the middle point and the two nearest points from the preceeding iteration. When the difference of the new value of maximum slope and the previous calculated maximum slope is less than $EP1$, a program input, the slope is accepted as the maximum. Then the values of time, slope and input parameters are printed out.

1. The first part of the document discusses the importance of maintaining accurate records of all transactions and the role of the accounting department in ensuring the integrity of the financial statements. It also highlights the need for regular audits and the importance of transparency in financial reporting.

2. The second part of the document focuses on the implementation of internal controls to prevent fraud and ensure the accuracy of financial data. It outlines the key components of a robust internal control system, including segregation of duties, authorization procedures, and regular monitoring and evaluation.

3. The third part of the document addresses the challenges faced by organizations in managing their financial resources effectively. It discusses the importance of budgeting and forecasting, and the role of the accounting department in providing accurate and timely financial information to management for decision-making.

4. The fourth part of the document discusses the impact of technology on the accounting profession. It highlights the benefits of using accounting software and the importance of staying up-to-date with the latest technological advancements in the field.

5. The fifth part of the document discusses the role of the accounting department in ensuring compliance with relevant laws and regulations. It emphasizes the importance of staying up-to-date with changes in the regulatory environment and the need for a strong compliance framework.

6. The sixth part of the document discusses the importance of communication and collaboration between the accounting department and other departments within the organization. It highlights the need for clear lines of communication and the importance of working together to achieve the organization's financial goals.

7. The seventh part of the document discusses the role of the accounting department in providing financial advice to management. It highlights the importance of providing accurate and timely financial information and the need for a strong relationship between the accounting department and management.

8. The eighth part of the document discusses the importance of maintaining accurate records of all transactions and the role of the accounting department in ensuring the integrity of the financial statements. It also highlights the need for regular audits and the importance of transparency in financial reporting.

9. The ninth part of the document discusses the implementation of internal controls to prevent fraud and ensure the accuracy of financial data. It outlines the key components of a robust internal control system, including segregation of duties, authorization procedures, and regular monitoring and evaluation.

10. The tenth part of the document addresses the challenges faced by organizations in managing their financial resources effectively. It discusses the importance of budgeting and forecasting, and the role of the accounting department in providing accurate and timely financial information to management for decision-making.

TABLE 1. INDEPENDENCE OF SLO3 AND SLO5 FROM G

PROGRAM	G	NTU	SLOPE x NTU	TIME AT MAX. SLOPE		
SL05	0.0	5	.68803355	3.39803		
SL05	0.1	5	.68803300	3.39796		
SL03	-0.1	10	.92857109	8.45713		
SL03	0.0	10	.92857102	8.45713		
SL03	0.1	10	.92857099	8.45713		
SL05	-0.1	10	.92857093	8.45713		
SL05	0.0	10	.92857086	8.45713		
SL05	0.1	10	.92857097	8.45713		
SL03	0.0	20	1.28623734	18.48003		
SL03	0.1	20	1.28623734	18.48003		
SL05	0.0	50	2.00992025	48.49231		
SL05	0.1	50	2.00992025	48.4923		
SL03	0.0	100	2.8316134	98.49618		
SL03	0.1	100	2.8316134	98.49610		
TEST FOR SUFFICIENT NUMBER OF PARTIAL SUMS						
PROGRAM	PARTIAL SUMS	SLOPE x NTU	TIME AT MAX. SLOPE	NTU		
SL03	25	.68803060	3.39793	5		
SL03	95	.68803060	3.39793	5		
SL05	20	1.28623734	18.47998	20		
SL05	50	1.28623734	18.47999	20		
SL05	1000	1.28623734	18.48001	20		
SL03	20	2.00992025	48.49231	50		
SL03	50	2.00992025	48.49234	50		
SL03	100	2.00992025	48.49234	50		

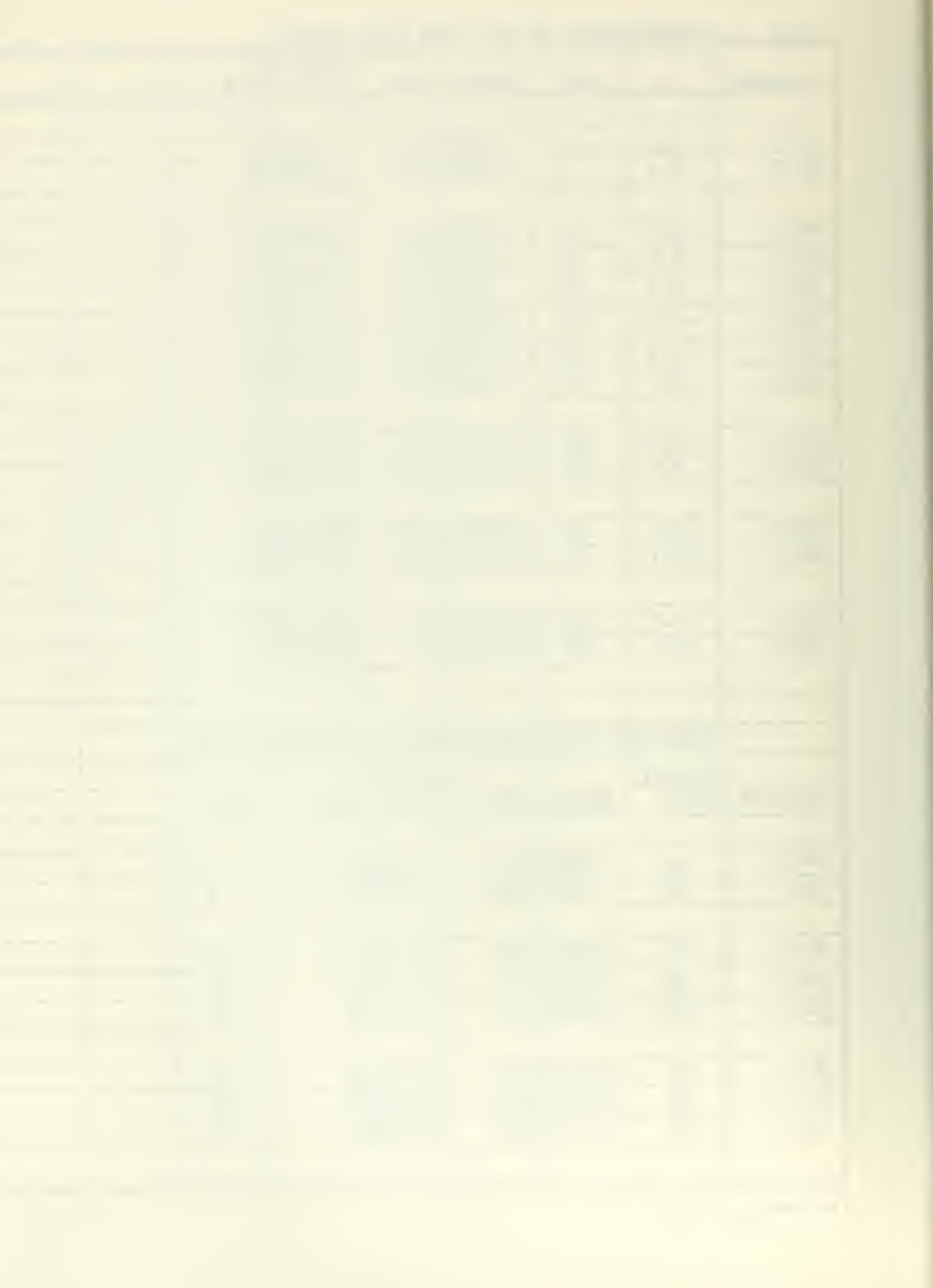


TABLE 2. RESULTS OF SLO3 AND SLO5 FOR $\lambda = 0.0$

[illegible]

TABLE 3. INDEPENDENCE OF SLO5 FROM G FOR $\lambda = .04$

PROGRAM	G	NTU	SLOPE x NTU	TIME AT MAX. SLOPE		
SL05	0.0	10	.89545795	7.43133		
SL05	0.1	10	.89545744	7.43132		
COMPARISON OF SL03 AND SL05						
SL03	0.0	10	.89545690	7.43140		
SL05	0.0	10	.89545795	7.43133		
TEST FOR SUFFICIENT NUMBER OF PARTIAL SUMS						
PROGRAM	PARTIAL SUMS	SLOPE x NTU	TIME AT MAX. SLOPE	NTU		
SL05	20	.89545795	7.43133	10		
SL05	50	.89545795	7.43138	10		
SL05	100	.89545795	7.43136	10		
RESULTS OF SL05 FOR $\lambda = 0.04$						
NTU	PROGRAM	SLOPE x NTU	TIME AT MAX. SLOPE	CPH SOLUTION	TIME AT MAX. SLOPE	% DIFF. OF CPH COMPARED TO SL05
2	SL05	.60485	.18037	.548	—	-9.42
5	SL05	.70586	3.05083	.704	—	-0.26
10	SL05	.89546	7.43133	.88926	7.404	-0.69
20	SL05	1.09744	16.18859	1.08959	16.164	-0.72
50	SL05	1.31977	42.61899	1.31301	42.696	-0.51
100	SL05	1.42976	87.02667	—	—	—
COMPUTATION TIME						
8 to 15 minutes/search						

TABLE 4. RESULTS OF SLO2 AND SLO4 FOR $\lambda = 0.0$

NTU=10/G	PROGRAM	SLOPE x NTU	GRAPHICAL BEST G	GRAPHICAL SLOPE x NTU	R. MAXIM SOLUTION	% DIFF. OF SLO2 & SLO4 COMPARED TO MAXIM
G:						
.056	SLO4	.93855415				
.056	SLO2	.93823756				
	mean	.93839585	.0585	.9389	.929	+1.07
NTU = 20						
G:						
.036	SLO4	1.30535030				
.036	SLO2	1.30625902				
	mean	1.30580966	.03475	1.3042	1.286	+1.38
NTU = 50						
G:						
.0125	SLO4	2.02431970				
.0125	SLO2	2.02571720				
	mean	2.02501895	.01175	2.0195	2.010	+0.47
NTU = 100						
G:						
0.0	SLO4	2.7173475				
.0125	SLO2	3.0172562				
	mean	2.8673018	.0055	2.825	—	—
NTU = 5						
G:						
0.0	SLO4	.69081005				
.03	SLO2	.69395495				
	mean	.6923825	-.045	.6905	.688	+0.36
NTU = 2						
G:						
0.0	SLO4	.5226				
0.0	SLO2	.5078				
	mean	.5152	—	—	.541	-4.80

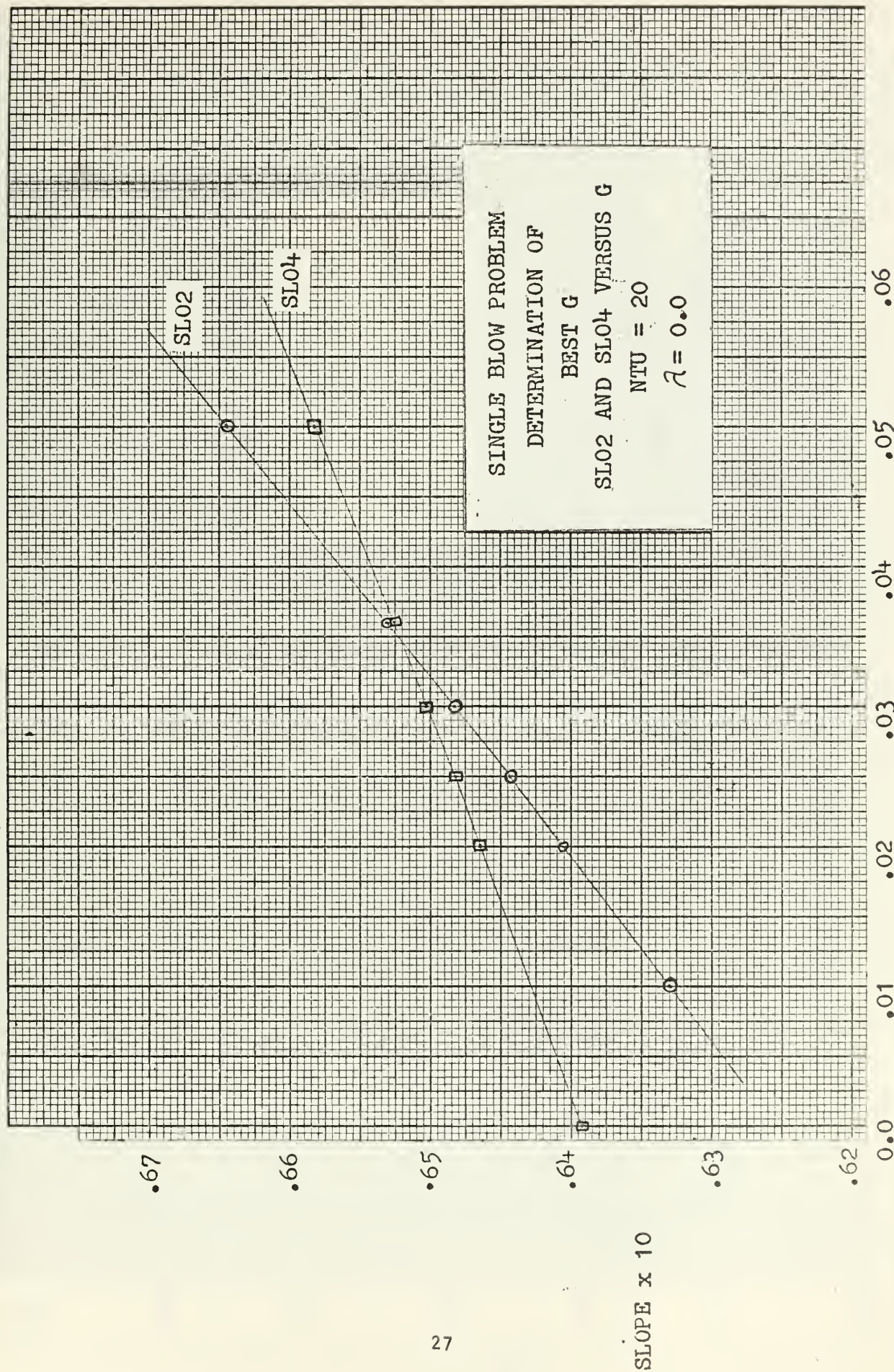


FIGURE 5

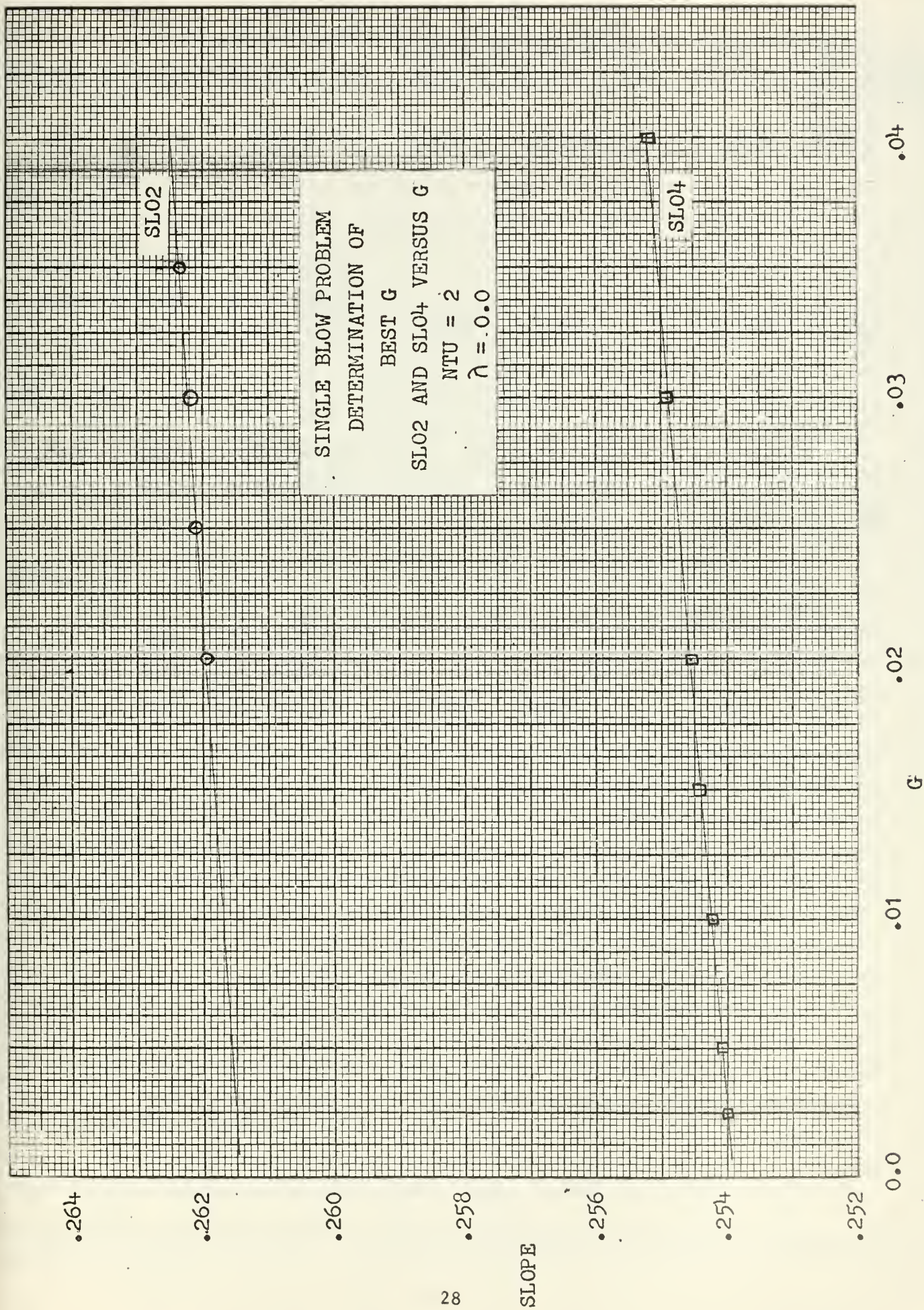


FIGURE 6

TABLE 5. RESULTS OF SLO2 AND SLO4 FOR $\lambda = 0.005$

[illegible]

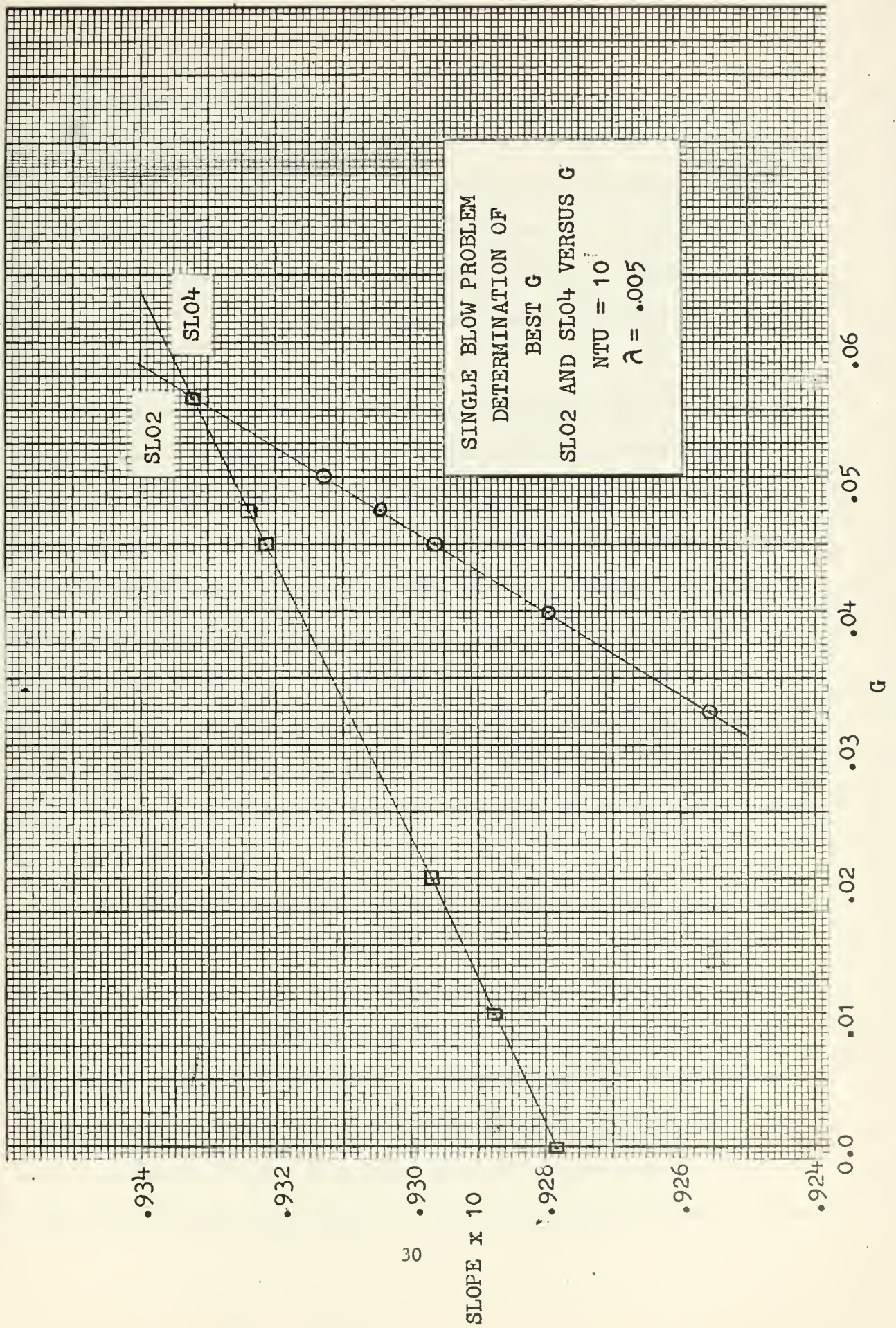


FIGURE 7

6. Discussion of Results.

Table 1 indicates that programs SLO3 and SLO5 are not sensitive to G and that both programs give the same solution to six decimal places for NTU greater than 5. The variation of G from -0.1 to +0.1 is much larger than the variations used in the SLO2 and SLO4 programs which are more sensitive to G . All results presented were calculated with eight point formulas.

One way to increase the accuracy of the program is to increase the number of terms in the partial sum. There is a test in the program which will increment the number of partial sums if the n th average has not converged to within 1×10^{-9} of the preceeding n th average for each calculation of slope. The test for the sufficient number of partial sums indicates that for NTU greater than five, twenty partial sums will give the same accuracy as 100 partial sums for programs SLO3 and SLO5. At NTU of five, the SLO3 program automatically increased the number of partial sums to 25 which then gave as accurate a solution as 95 partial sums. There is an indication that for lower values of NTU, more partial sums may be necessary.

R. E. Maxim^[10] presented a table of values of maximum slopes calculated with Schumann's solution for the special case of $\lambda = 0.0$. Schumann's solution is an infinite series of Bessel functions. Each value of slope was calculated using Bessel functions accurate to ten significant places and the summation was continued until there was no change in the tenth decimal place of the solution. Unfortunately, the search by Maxim could not distinguish between relative maximum slope values and his search ended when the slope at the next increment of time

was less than the preceeding slope. Relative maximum slopes have been found by the theoretical solution presented in this paper and their existence is supported by experimental evidence found by J. M. Bannon [1], Figure 26. The results of Table 2 clearly indicate that Maxim's values, though accurate to six places, were calculated at a time much too low to have found the largest relative maximum slope in the NTU range less than five. For values of NTU equal to and greater than five, both the time at which maximum slope occurred and the values of maximum slope times NTU calculated by SL03 agree to at least seven decimal places with Maxim's results. SL05 solutions were in complete agreement with the results of SL03.

The computation time depends on the degree of accuracy required to calculate one value of slope. The accuracy required of the search routine for the results of Table 2 was $\pm 1 \times 10^{-9}$ difference in the new value of maximum slope as compared to the previous iteration. For values of NTU less than ten, the number of iterations required was four or five times the number for NTU values greater than ten. Once the approximate value of time at maximum slope is known, the search routine can be set to find the maximum with fewer iterations. But, even without optimum starting times the computation time was approximately half a minute for the $\lambda = 0.0$ case. For non zero values of λ , the computation time per search is expected to be twelve minutes.

Results of SL05 for $\lambda = .04$ are shown to be insensitive to G in Table 3. One test point at NTU = 10 indicates good agreement between SL05 and SL03 programs. As for the $\lambda = 0$ case, results indicate good agreement with C. P. Howard's results [5]. For NTU greater than five Howard's results are consistantly low but all have less than 1% difference as compared to SL05. As in the $\lambda = 0$ case, Howard's results for

NTU equal to two are much lower than those obtained by SLO5. Again this is probably a failure of his search technique to distinguish between relative maximum slopes. Unfortunately, he did not publish the times at which the maximum slopes occurred. Howard also used the incremental step search and the search ended when the newly calculated slope was less than the preceeding slope.

Programs SLO2 and SLO4 are quite sensitive to parameter G. The results obtained graphically and listed in Table 4 were compared to the accurate solution of Maxim for $\lambda = 0.0$. The percent error of the graphical results was less than $\pm 1.5\%$ except at NTU = 2. Figure 6 indicates that this intercept was not determined. Considerable effort would be required to find this intercept and obviously the mean value at NTU = 2 has unacceptably large error. For the other values of NTU, however, intercepts were easily found as indicated by Figure 5.

Table 5 shows similar results for $\lambda = 0.005$. No accurately known values are available for this region. C. P. Howard's results are compared to the results obtained by SLO2 and SLO4. If as expected, the SLO2 and SLO4 results are 1 to 1.5% too large, then C. P. Howard's solutions for $\lambda = 0.005$ would be approximately .5% too low for NTU greater than 10. Figure 7 again shows how the intercept or best G was obtained.

7. Conclusions and Recommendations.

Program SL05, using the VR, Gauss-Legendre formulas, is a fast accurate tool capable of supplying all the theoretical maximum slope data needed for experimental testing of compact heat exchanger surfaces. The SL03, VI, program is equally accurate but slightly slower. The SL05 program is being applied to verify the NTU versus Maximum Slope curves presented by C. P. Howard [5]. The results of these calculations will be published at a later date.

The combination of Laplace transforms with numerical inversion should be applicable to most boundary value problems in which one is able to express the solution as an inverse Laplace transform. Therefore, this technique is primarily limited in application to linear systems of partial differential equations with constant coefficients.

The two main problems encountered in the numerical inversion were the slow convergence of the integration and radical behavior of the function of s at time equal zero. The VR and VI functions were cyclic in nature with slowly decreasing magnitudes and period. For this particular solution the Legendre polynomial approximated the functions better than Chebyshev's polynomial. However, for other functions a number of other polynomials may give better results. The acceleration of convergence is adequately accomplished by the present numerical inversion but it generates a problem in addition. Because of the averaging technique applied to the partial sums to accelerate convergence the formal error analysis normally applied to each partial sum is impossible. Therefore, the only way remaining to determine the accuracy of the calculated maximum slopes was by comparison with R. E. Maxim's accurately determined values for the

limiting case of $\lambda = 0$. Even though direct inversion of the Laplace transform was possible for this case, the numerical inversion was accomplished in seconds with the same accuracy attained by the approximation to an infinite sum of Bessel functions carried out to six decimal place accuracy. For non-zero λ , there were no accurate solutions with which to compare. For these values an indication of accuracy was obtained by calculating the same points with an independent program. The SLO3 program is not independent of SLO5 in a strict interpretation of independence. However, they are different programs, SLO3 using the imaginary part of the inversion integral and SLO5 using the real part. Either program should give the same result. The same result to six or seven decimal places was obtained with these programs indicating excellent accuracy for a numerical process. The comparison of SLO5 results with Howard's results, obtained with a rather crude finite-difference technique, indicated that he obtained very accurate results by judicious application of the finite-difference technique. Most of his results were less than one half of one percent low when compared to SLO5.

The following recommendations indicate avenues of investigation that could be undertaken with either computer programs developed in conjunction with this thesis or the mathematical technique presented.

It is recommended that the temperature programs TEMP4 and TEMP2 be applied to obtain a time-temperature history for comparison with corresponding experimental results to determine how well the mathematical model represents the behavior of the experimental test rig.

An investigation should be conducted to determine the cause of and physical significance of the relative maximum slopes obtained both experimentally and theoretically for the heating cycle. One objective would be

to determine if the relative maximum obtained experimentally correspond in magnitude and time of occurrence with those obtained by theory. Experimentally it was noted that the relative maximums are practically indistinguishable for the cooling of the solid, but that for the same matrix and mass flow of fluid the relative maximums are very distinct for the case of heating the solid. An investigation should be made to determine theoretically the effect of longitudinal conduction for the cooling cycle as compared to the present solution for the heating cycle. The objective of this investigation would be to determine if the theoretical solution is capable of predicting a difference in response on cooling as compared to heating. The cooling cycle solution would require appropriate sign changes in the heat balance from which governing partial differential equations were derived. This may, therefore, require a new solution for cooling since the sign changes could cause a change in the auxiliary cubic equation 3b of Section 3. It is possible that a sign change of a term in this equation could cause a change in the significance of the parameter λ on the result of fluid temperature or slope of fluid temperature. Bannon [1] has noted experimentally that the largest maximum slope obtained by cooling agreed fairly well with that obtained by heating.

The theoretical results, in the region of $NTU = 2$, are difficult to obtain, and the determination of NTU given an experimental maximum slope in this NTU region is impossible. An attempt should be made to develop a curve matching technique employing a least square error method. This method would use three or more values of time and their corresponding temperatures from an experimental time-temperature history. The TEMP4 program would calculate theoretical values of temperature at the given

times for an estimated value of NTU. Then an NTU search routine could calculate the sum of the squared error of each temperature. After repeating this operation for two bracketing values of NTU, a Lagrange iteration method would calculate the NTU with the least squared error. Another possible means of curve matching would be to match the dimensionless time at which the maximum slope occurs for the region of $NTU = 2$, rather than matching the magnitudes of maximum slope. This would require an adequate starting mark on the experimental time-temperature history and a correction of the time at the maximum slope to account for the system time delay of the experimental response.

A more general system of governing partial differential equations can be obtained from the heat balance as derived by Creswick, by including a term to represent the energy stored in the fluid. This term is required for transient heat transfer testing using a liquid rather than a gas. The result of this addition changes equation 2 of section 3 to the following

$$\frac{\partial \nu}{\partial X} = \frac{1}{NTU} \left[u - \nu - \lambda_f \frac{\partial \nu}{\partial t} \right],$$

where $\lambda_f \triangleq \frac{\gamma C_f A_f \ell}{W_s C_s}$, the dimensionless fluid capacitance, and γ is the density of the fluid in lb/ft.³ This equation combined with Equation 1 of Section 3 would then be the new governing partial differential equations. The present mathematical technique should be capable of solving this system of equations.

BIBLIOGRAPHY

1. Bannon, J. M., "An Experimental Determination of Heat Transfer and Flow Characteristics of Perforated Material for Compact Heat Exchanger Surfaces," Master Thesis, 1964, U. S. Naval Postgraduate School.
2. Churchill, R. V., Operational Mathematics, McGraw-Hill, 1958, second edition.
3. Creswick, F. A., "A Digital Computer Solution of the Equations for Transient Heating of a Porous Solid Including the Effects of Longitudinal Conduction," Industrial Mathematics, 1957, pp. 61-69.
4. Franklin, P. Methods of Advanced Calculus, McGraw-Hill, 1944.
5. Howard, C. P., "Heat Transfer and Flow Friction Characteristics of Skewed Passage and Glass-Ceramic Heat Transfer Surfaces," Department of Mechanical Engineering, Stanford University, TR-No. 59, Appendix 3, pp. 31-43., Oct., 1963.
6. Hurwitz, H., Jr., and P. F. Sweifel, "Numerical Quadrature of Fourier Transform Integrals," Math Tables Aids Comp., X, 1956, pp. 140-149.
7. Jakob, M., Heat Transfer, Vol. II, John Wiley and Sons, Inc., 1957.
8. Lanczos, C., Applied Analysis, Prentice Hall, Inc., 1956.
9. Locke, G. L., "Heat Transfer and Flow-Friction Characteristics of Porous Solids," Department of Mechanical Engineering, Stanford University, TR-No. 10, June 1950.
10. Maxim, R. E., "Convective Heat Transfer and Flow Friction Characteristics of Compact Heat Exchanger Surfaces," Master Thesis, M386, 1962, U. S. Naval Postgraduate School.
11. Mondt, J. R., "Effects of Longitudinal Thermal Conduction in the Solid on Apparent Convection Behavior, with Data for Plate-Fin Surfaces," International Heat Transfer Conference, Boulder, Colorado, Paper No. 73, Proceedings, ASME, 1961.
12. Romie, F. E., et al., "Heat Transfer and Pressure Drop Characteristics of Four Regenerative Heat Exchanger Matrices," Department of Engineering, University of California, December 1948, Contract No. a(S)-8649 for Bureau of Aeronautics.
13. Schmittroth, L. A., "Numerical Inversion of Laplace Transforms," Communications of the ACM, pp. 171-172.

14. Schumann, T. E. W., "Heat Transfer: A Liquid Flowing Through a Porous Prism," Journal of Franklin Institute, CCVIII, July-December, 1929, pp. 405-416.

APPENDIX I

Solution for Zero and Infinite Longitudinal Conduction.

1. ZERO LONGITUDINAL CONDUCTIVITY

As in the solution for finite conductivity the development of this case is the same initially; cf, Equation 3a, page 8.

$$(1) \quad \frac{\partial^3 \nu(x,s)}{\partial x^3} + b \frac{\partial^2 \nu(x,s)}{\partial x^2} - \frac{b(s+1)}{a} \frac{\partial \nu(x,s)}{\partial x} - \frac{b^2}{a} s \nu(x,s) = 0$$

For this case where λ is defined as a , it is necessary to multiply by a .

The substitution of $a = 0$ results in the equation

$$(2) \quad \nu' + b \frac{s}{s+1} \nu = 0.$$

The general solution of equation 2 is

$$(3) \quad \nu(x,s) = C_1(s) e^{r_1 x} = C_1(s) e^{-\frac{b s}{s+1} x}.$$

The boundary conditions are the same as in the previous solution.

Boundary conditions a and b were applied in order to arrive at equation

1, above. Boundary condition c is $v(0,t) = C$ which transforms into $v(0,s) =$

C/s . Applying boundary condition c to equation 3 results in

$$\nu(0,s) = \frac{C}{s} = C_1(s), \quad \text{therefore}$$

$$(4) \quad \nu(x,s) = \frac{C}{s} e^{-\frac{b s}{s+1} x} \quad \text{and} \quad \nu(1,s) = \frac{C}{s} e^{-\frac{b s}{s+1}}$$

It follows directly,

$$(5) \quad \frac{\partial v}{\partial t}(x, s) = C e^{-\frac{b s}{s+1} x} \quad \text{and} \quad \frac{\partial v}{\partial t}(1, s) = C e^{-\frac{b s}{s+1}}.$$

This special case was solved analytically in 1929 by T. E. W. Schumann [14]. The following development will show that the present solution agrees with Schumann's.

Let $s' = s + 1$ and apply it to equation 4.

Then
$$v(x, s'-1) = \frac{C}{s'-1} e^{-b \frac{s'-1}{s'} x} \quad \text{or}$$

$$(6) \quad v(x, s'-1) = C e^{-bx} \sum_{m=1}^{\infty} e^{\frac{bx}{s'}} \frac{1}{s'^m}$$

From page 229 of reference [2], we find

$$(7) \quad \mathcal{L}^{-1} \left\{ \frac{1}{s^\mu} e^{\frac{\kappa}{s}} \right\} = \left(\frac{t}{\kappa} \right)^{\frac{\mu-1}{2}} I_{\mu-1} (2\sqrt{\kappa t}).$$

Comparing equation 6 and 7, the inverse transform of equation 6 becomes:

$$(8) \quad \mathcal{L}^{-1} \{ v(x, s') \} = C e^{-bx} \sum_{m=1}^{\infty} \left(\frac{t}{bx} \right)^{\frac{m-1}{2}} I_{m-1} (2\sqrt{btx}).$$

From page 294 [2] is

$$\mathcal{L}^{-1} \{ f(s-a) \} = e^{at} \cdot \mathcal{L}^{-1} \{ f(s) \} \quad \text{therefore,}$$

$$(9) \quad v(x, t) = C e^t e^{-bx} \sum_{m=1}^{\infty} \left(\frac{t}{bx} \right)^{\frac{m-1}{2}} I_{m-1} (2\sqrt{btx}),$$

$$(9a) \quad v(x, t) = C e^{-b(x-\frac{t}{b})} \sum_{m=0}^{\infty} \left(\frac{t}{bx} \right)^{\frac{m}{2}} I_m (2\sqrt{btx}).$$

Define $a = btx$ and $W = 2\sqrt{a}$, then compare equation 9a with the form

$$(9b) \quad a^{-\frac{m}{2}} I_m(2\sqrt{a}).$$

Note that

$$(9c) \quad \left(\frac{t}{bx}\right)^{\frac{m}{2}} = \frac{t^m}{(bxt)^{m/2}} = t^m a^{-\frac{m}{2}}$$

Equation 9a then becomes

$$(10) \quad w(x,t) = C e^{-bx+t} \sum_{m=0}^{\infty} t^m a^{-\frac{m}{2}} I_m(2\sqrt{a}).$$

Schumann's solution is

$$(11) \quad w(y,z) = e^{-y-z} \sum_{m=0}^{\infty} z^m \frac{d^m J_0(2i\sqrt{yz})}{d(yz)^m}.$$

Equations 10 and 11 are equivalent which can be shown as follows. From page 392 [4], the modified Bessel function identity is

$$\frac{d}{dW} [W^{-m} I_m(W)] = W^{-m} I_{m+1}(W) \quad \text{where } m \geq 0$$

Then, for $n = 0$ and $W = 2\sqrt{a}$,

$$\frac{d}{dW} [I_0(W)] = I_1(W)$$

Apply the chain rule such that

$$\frac{d[Y]}{da} = \frac{dY}{dW} \cdot \frac{dW}{da}$$

It follows that

$$\frac{d[I_0(2\sqrt{a})]}{da} = a^{-1/2} I_1(2\sqrt{a}).$$

By mathematical induction it can be shown that

$$(12) \quad \frac{d^m}{da^m} [I_0(2\sqrt{a})] = a^{-\frac{m}{2}} I_m(2\sqrt{a}).$$

Equation 10 then becomes

$$(13) \quad W(x,t) = (e^{-bx+t} \sum_{m=0}^{\infty} t^m \frac{d^m}{da^m} [I_0(2\sqrt{a})])$$

From page 392 [4] ,

$$I_m(2\sqrt{a}) = i^{-m} J_m(2i\sqrt{a}), \text{ and} \\ I_0(2\sqrt{a}) = J_0(2i\sqrt{a}).$$

Note that Schumann's development is for the case of heating the fluid as time increases and that the present case is developed for cooling of the fluid with increasing time, which changes the sign of t in the exponential term . It then follows that equation 13 is, indeed,

$$(11) \quad W(y,z) = e^{-y-z} \sum_{m=0}^{\infty} z^m \frac{d^m}{d(yz)^m} [J_0(2i\sqrt{yz})].$$

Since the program for numerical inversion of equations 5 and 6 is already available it is much easier and probably much faster to apply it than to evaluate equation 11. The same theoretical solution was obtained by G. L. Locke in 1950 [9] .

2. INFINITE LONGITUDINAL CONDUCTIVITY

When $\lambda = \infty$, the solid temperature is no longer a function of x . In fact the following is true: $\frac{\partial^m u}{\partial x^m}(x, t) = 0$. Therefore, equation 1, page 7, becomes indeterminate and must be replaced by:⁷

$$(1) \quad \frac{du(t)}{dt} = \int_0^1 [v(x, t) - u(t)] dx \quad \text{and equation 2 is}$$

$$(2) \quad \frac{\partial v}{\partial x}(x, t) = NTU [u(t) - v(x, t)] .$$

The boundary conditions to be applied to this case are:

- a. $v(x, 0) = 0$,
- b. $v(x, 0) = 0$, and
- c. $v(0, s) = C/s$.

Solve equation 2 for $u(t)$ and take the derivative of u with respect to t . Then substituting these back into equation 1 and applying boundary condition c, results in

$$\begin{aligned} \frac{1}{NTU} \frac{\partial^2 v}{\partial x \partial t}(x, t) + \frac{\partial v}{\partial t}(x, t) &= \int_0^1 \left[v(x, t) - \frac{1}{NTU} \frac{\partial v}{\partial x}(x, t) - v(x, t) \right] dx \\ &= \frac{-1}{NTU} [v(1, t) - C] . \end{aligned}$$

Multiply through by NTU and rearrange the terms to arrive at

$$(3) \quad \frac{\partial^2 v}{\partial x \partial t}(x, t) + NTU \frac{\partial v}{\partial t}(x, t) + v(1, t) - C = 0 .$$

Transformation of each term in 3 by Laplace gives

⁷For further discussion, see page 47.

$$(4) - \frac{\partial v}{\partial x}(x,0) + S \frac{\partial v}{\partial x}(x,S) + NTU[-v(x,0) + S v(x,S)] + v(1,S) - \frac{C}{S} = 0$$

Applying boundary conditions a and b and dividing by s, equation 4 reduces to

$$(5) \quad \frac{\partial v}{\partial x}(x,S) + NTU v(x,S) = \frac{C}{S^2} - \frac{v(1,S)}{S}.$$

Again by treating s as a parameter, equation 5 is a total differential equation. The solution of the differential equation is

$$(6) \quad v(x,S) = C_1(s) e^{-(NTU)x} + \frac{1}{NTU} \cdot \frac{1}{S} \left[\frac{C}{S} - v(1,S) \right].$$

Now apply boundary condition c to equation 6 which results in

$$(7) \quad v(0,S) = \frac{C}{S} = C_1(s) + \frac{1}{NTU} \cdot \frac{1}{S} \left[\frac{C}{S} - v(1,S) \right]$$

Therefore, $C_1(s) = \frac{C}{S} \left[1 - \frac{1}{NTU \cdot S} \right] + \frac{1}{NTU \cdot S} v(1,S)$, and

$$(8) \quad v(x,S) = \frac{C}{S} e^{-NTU \cdot x} + \frac{1}{NTU \cdot S} \left[\frac{C}{S} - v(1,S) \right] (1 - e^{-NTU \cdot x})$$

Solve equation 8 for v(1,s) as follows:

$$v(1,S) = \frac{C}{S} e^{-NTU} + \frac{1}{NTU \cdot S} \left[\frac{C}{S} - v(1,S) \right] (1 - e^{-NTU})$$

$$v(1,S) \left[1 + \frac{(1 - e^{-NTU})}{NTU \cdot S} \right] = \frac{C}{S} \left[\frac{(1 - e^{-NTU})}{NTU \cdot S} + e^{-NTU} \right].$$

Define $\xi = \frac{(1 - e^{-NTU})}{NTU}$; then $e^{-NTU} = 1 - \xi NTU$, and

$$(9) \quad W(1, S) = \frac{C}{S} \frac{(1 + \frac{\xi}{S} - \xi \cdot NTU)}{(1 + \xi/S)}$$

The particular fluid temperature of interest is that temperature at $x = 1$.

Also the value of C must be dimensionless, for comparison with Mondt's solution, and can be set equal to one. It follows directly that

$$W(1, S) = \frac{1 (1 + \frac{\xi}{S} - \xi \cdot NTU)}{(S + \xi)}$$

$$(10) \quad W(1, S) = \frac{1}{S + \xi} - \frac{\xi \cdot NTU}{S + \xi} + \frac{\xi}{S(S + \xi)} .$$

The inverse Laplace transform of equation 10 is

$$W(1, t) = e^{-\xi t} - NTU \cdot \xi e^{-\xi t} + 1 - e^{-\xi t}$$

which reduces to

$$(11) \quad n(1,t) = 1 - NTU \int e^{-\xi t},$$

where $\xi = \frac{1 - e^{-NTU}}{NTU}$. The solution as a function of time is

$$n(1,t) = 1 - (1 - e^{-NTU}) e^{-\frac{(1 - e^{-NTU})}{NTU} t}.$$

This solution is in complete agreement with that derived by J. R. Mondt [11] in 1961. Since a convenient inverse transform was available it was unnecessary to apply the intricate numerical inversion.

To derive Equation (1) for this special case it was necessary to refer to the heat balance from which Creswick [3] derived the governing equations. The last term of Creswick's Equation (1) was eliminated and the remaining terms were arranged in terms of dimensionless parameters. Then both sides of the equation were integrated over the length of the matrix to arrive at Equation (1) on page 44.

APPENDIX II

Flow diagrams and program listings.

The flow diagrams will precede the applicable program listings.

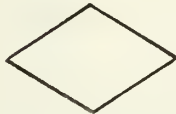
The symbols used in the flow diagrams are defined as follows:



Terminal - the beginning, end, or point of interruption in the program



Input/Output - input symbols are preceded by a terminal.



Decision - branches are labeled by sign according to the sign of the value enclosed.



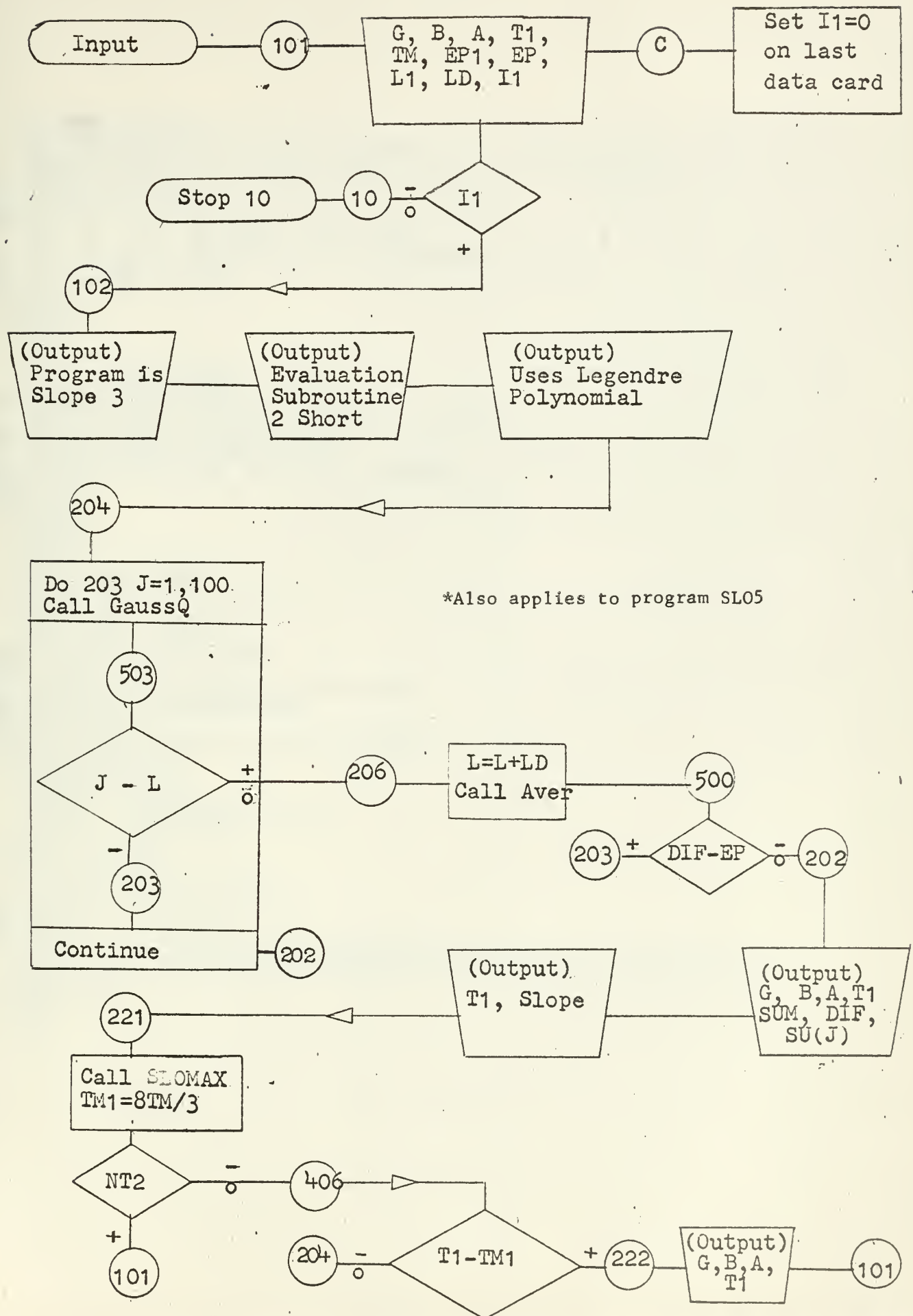
Connector - enclosed numbers refer to the prefix numbers of the corresponding statements on the program listing.



Offpage Connector - designates an entry to or exit from a page.

There are six distinct programs which are used separately, although they could be combined into a larger package to make use of one or another at the user's option. There are the four "slope" programs, SL02, SL03, SL04 and SL05 which have been described in detail in the body of the thesis, and the two "temperature" programs TEMP2 and TEMP4, which have been referred to in the text but not described in detail. The latter are intended to provide a time-temperature history; no use of these programs has been made in this thesis. See page 35 for recommendations concerning their use.

PROGRAM SLO3*



*Also applies to program SLO5


```

PROGRAM SLO3
DIMENSION VR(20),VI(20),SU(200),AV(12,10),R(129),X(129),ER(200),
1RR(128),RI(128),T(10),SLO(10)
COMMON RR,RI,T,SLO,G,R,A,PI,SLOPE,NT,NT1,NT2,EP1,I1,T1
COMMON NT3,TM
101 READ 100,G,B,A,T1,TM,EP1,EP,L1,LD,I1
100 FORMAT(7F10.5,3I3)
C SET I1 = 0 ON LAST DATA CARD
C I1 IS THE AVERAGE AND THE POLYNOMIAL ORDER
IF(I1)10,10,102
102 CONTINUE
NT=-1
NT2=0
K=1
NT1=-1
PI=3.1415926536
WRITE OUTPUT TAPE 4,301
301 FORMAT(24H PROGRAM IS SLOPE 1, N=8/)
WRITE OUTPUT TAPE 4,302
302 FORMAT(30H EVALUATION SUBROUTINE 2 SHORT/)
WRITE OUTPUT TAPE 4,305
305 FORMAT(25H USES LEGENDRE POLYNOMIAL/)
204 L=L1
NT3=-1
SU=0.
D=0.0
E=1.0
DO 203 J=1,100
CALL GAUSSQ(D,E,VAL)
D=D+1.0
E=E+1.0
SU(J)=VAL+SU(J-1)
503 IF(J-L)203,206,206
206 L=L+LD
CALL AVER(SU,AV,I1,J,DIF,SUM)
500 IF(DIF-EP)202,202,203
203 CONTINUE
CALL AVER(SU,AV,8,100,DIF,SUM)
202 EG=EXP(-G*T1)
EG2=2.*EG/T1
SLOPE=EG2*SUM
PRINT 3,G,B,A,T1
PRINT 4,SUM,DIF,J,SU(J)
PRINT 2,T1,SLOPE
221 CALL SLOMAX
TM1=8.*TM/3.
IF(NT2)406,406,101
406 IF(T1-TM1)204,204,222
222 PRINT 3,G,B,A,T1
2 FORMAT(3H T=F10.5,3X,6HSLOPE=E20.8/)
3 FORMAT(3H G=F10.5,3X,2H B=F10.5,3X,2H A=F10.5,3X,2H T=F10.5/)
4 FORMAT(5H SUM=E20.8,3X,4H DIF=F10.9,3X,3H SU(13,2H)=E20.8/)
GO TO 101
10 STOP 10
END

```

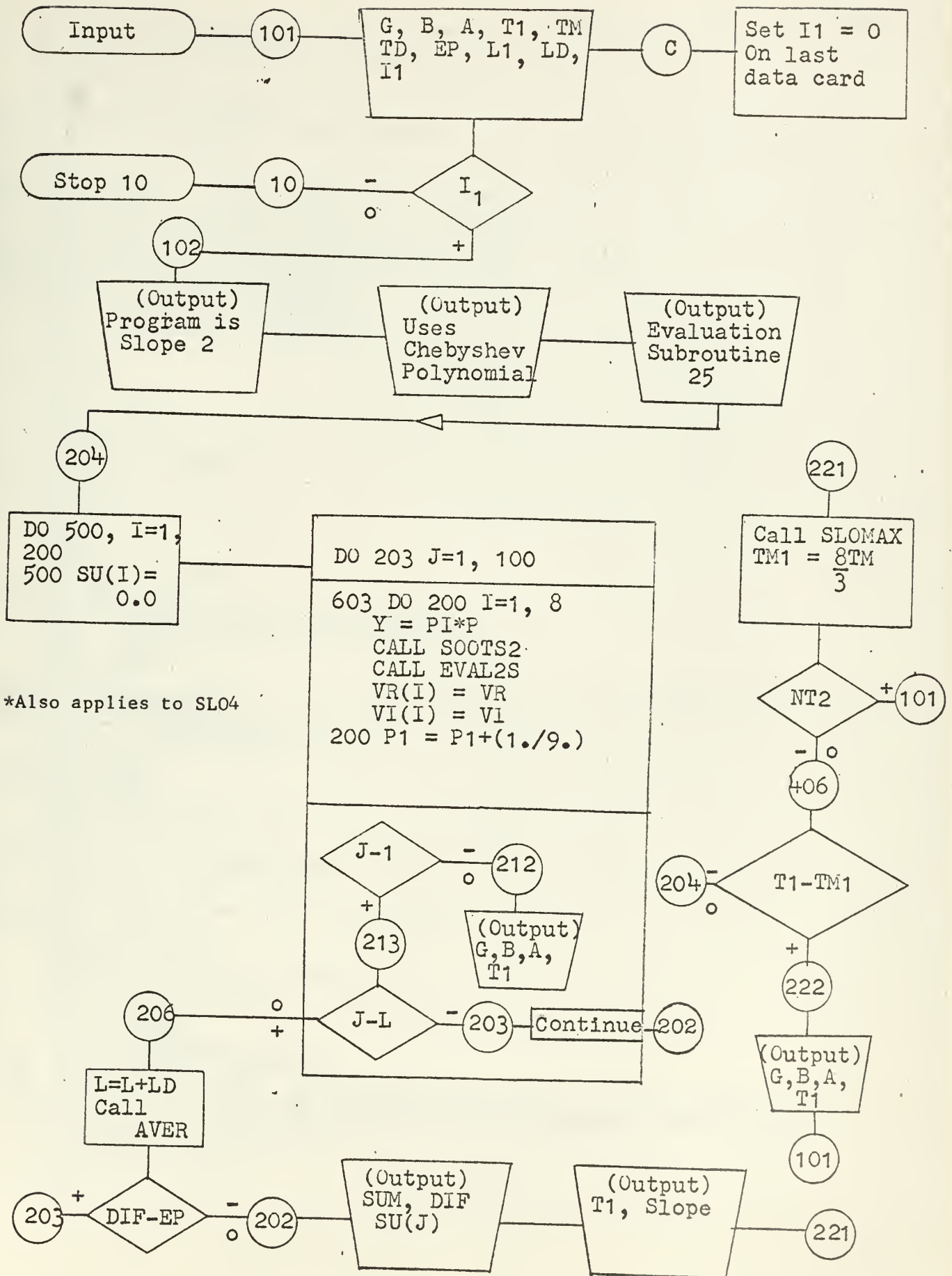


```

PROGRAM SLO5
DIMENSION VR(20),VI(20),SU(200),AV(12,10),R(129),X(129),ER(200),
1RR(128),RI(128),T(10),SLO(10)
COMMON RR,RI,T,SLO,G,B,A,PI,SLOPE,NT,NT1,NT2,EP1,I1,T1
COMMON NT3,TM
101 READ 100,G,B,A,T1,TM,EP1,EP,L1,LD,I1
100 FORMAT(7F10.5,3I3)
SET I1 = 0 ON LAST DATA CARD
I1 IS THE AVERAGE AND THE POLYNOMIAL ORDER
IF(I1)10,10,102
102 CONTINUE
NT=-1
NT2=0
K=1
NT1=-1
PI=3.1415926536
WRITE OUTPUT TAPE 4,301
301 FORMAT(24H PROGRAM IS SLOPE 5, N=8/)
WRITE OUTPUT TAPE 4,302
302 FORMAT(30H EVALUATION SUBROUTINE 2 SHORT/)
WRITE OUTPUT TAPE 4,305
305 FORMAT(25H USES LEGENDRE POLYNOMIAL/)
204 L=L1
NT3=-1
SU=0.
D=0.0
E=1.0
DO 203 J=1,100
CALL GAUSSQ(D,E,VAL)
D=D+1.0
E=E+1.0
SU(J)=VAL+SU(J-1)
503 IF(J-L)203,206,206
206 L=L+LD
CALL AVER(SU,AV,I1,J,DIF,SUM)
500 IF(DIF-EP)202,202,203
203 CONTINUE
CALL AVER(SU,AV, 8,100,DIF,SUM)
202 EG=EXP(-G*T1)
EG2=2.*EG/T1
SLOPE=EG2*SUM
PRINT 3,G,B,A,T1
PRINT 4,SUM,DIF,J,SU(J)
PRINT 2,T1,SLOPE
221 CALL SLOMAX
TM1=8.*TM/3.
IF(NT2)406,406,101
406 IF(T1-TM1)204,204,222
222 PRINT 3,G,B,A,T1
2 FORMAT(3H T=F10.5,3X,6HSLOPE=E20.8/)
3 FORMAT(3H G=F10.5,3X,2HE=F10.5,3X,2HA=F10.5,3X,2HT=F10.5/)
4 FORMAT(5H SUM=E20.8,3X,4HDIF=F10.9,3X,3HSU(13,2H)=E20.8/)
GO TO 101
10 STOP 10
END

```


PROGRAM SLO2*



*Also applies to SLO4


```

PROGRAM SLO2
DIMENSION RR(128),RI(128),VI(20),VR(20),SU(200),AV(12,10),R(129),
IX(129),SLO(10),T(10)
COMMON SLOPE,SLO,T,NT,NT1,NT2,K,EP1,G,B,A,PI,T1,TM
COMMON NT3
101 READ 100,G,B,A,T1,TM,TD,EP,L1,LD,I1
100 FORMAT(7F10.5,3I3)
C SET I1 = 0 ON LAST DATA CARD
IF(I1)10,10,102
102 C1=1.0
210 WRITE OUTPUT TAPE 4,301
301 FORMAT(24H PROGRAM IS SLOPE 2, N=4)
WRITE OUTPUT TAPE 4,304
304 FORMAT(26H USES CHEBYSHEV POLYNOMIAL)
401 WRITE OUTPUT TAPE 4,302
302 FORMAT(30H EVALUATION SUBROUTINE 2S /)
W1C=.10776070/.98480775
W2C=.083333333/.86602540
W3C=.045908434/.64278761
W4C=.012997531/.34202014
NT=-1
NT1=-1
NT2=0
K=1
EP1=.000001
NT3=-1
204 P=3.1415926536/T1
DO 500 I=1,200
500 SU(I)=0.0
L=L1
P1=1./9.
SGN=-1.
SU=0.
DO 203 J=1,100
603 DO 200 I=1,8
Y=P1*P
CALL SOOTS2 (G,B,A,Y,R,X,RR,RI)
CALL EVAL2S(RR,RI,G,B,Y,C1,VR,VI)
VR(I)=VR
VI(I)=VI
200 P1=P1+(1./9.)
605 SU(J)=SGN*(W1C*(VI(4)+VI(5))+W2C*(VI(3)+VI(6))+W3C*(VI(2)+VI(7))+
1W4C*(VI(1)+VI(8)))+SU(J-1)
IF(J-1) 212,212,213
212 PRINT 3,G,B,A,T1
213 CONTINUE
SGN=-SGN
P1=P1+(2./9.)
IF(J-L)203,206,206
206 L=L+LD
CALL AVER(SU,AV,I1,J,DIF,SUM)
IF(DIF-EP)202,202,203
203 CONTINUE
CALL AVER(SU,AV,10,100,DIF,SUM)
202 EG=EXPFG*T1
EG2=2.*EG/T1
SLOPE=EG2*SUM
PRINT 4,SUM,DIF,J,SU(J)
PRINT 2,T1,SLOPE
221 CALL SLOMAX
TM1=8.*TM/3.
IF(NT2)406,406,101
406 IF(T1-TM1)204,204,222
222 PRINT 3,G,B,A,T1
2 FORMAT(3H T=F10.5,3X,6HSLOPE=E15.8//)
3 FORMAT(3H G=F10.5,3X,2HB=F10.5,3X,2HA=F10.5,3X,2HT=F10.5//)
4 FORMAT(5H SUM=E15.8,3X,4HDIF=F10.9,3X,3HSU(13,2H)=E15.8//)
GO TO 101
10 STOP 10
END

```

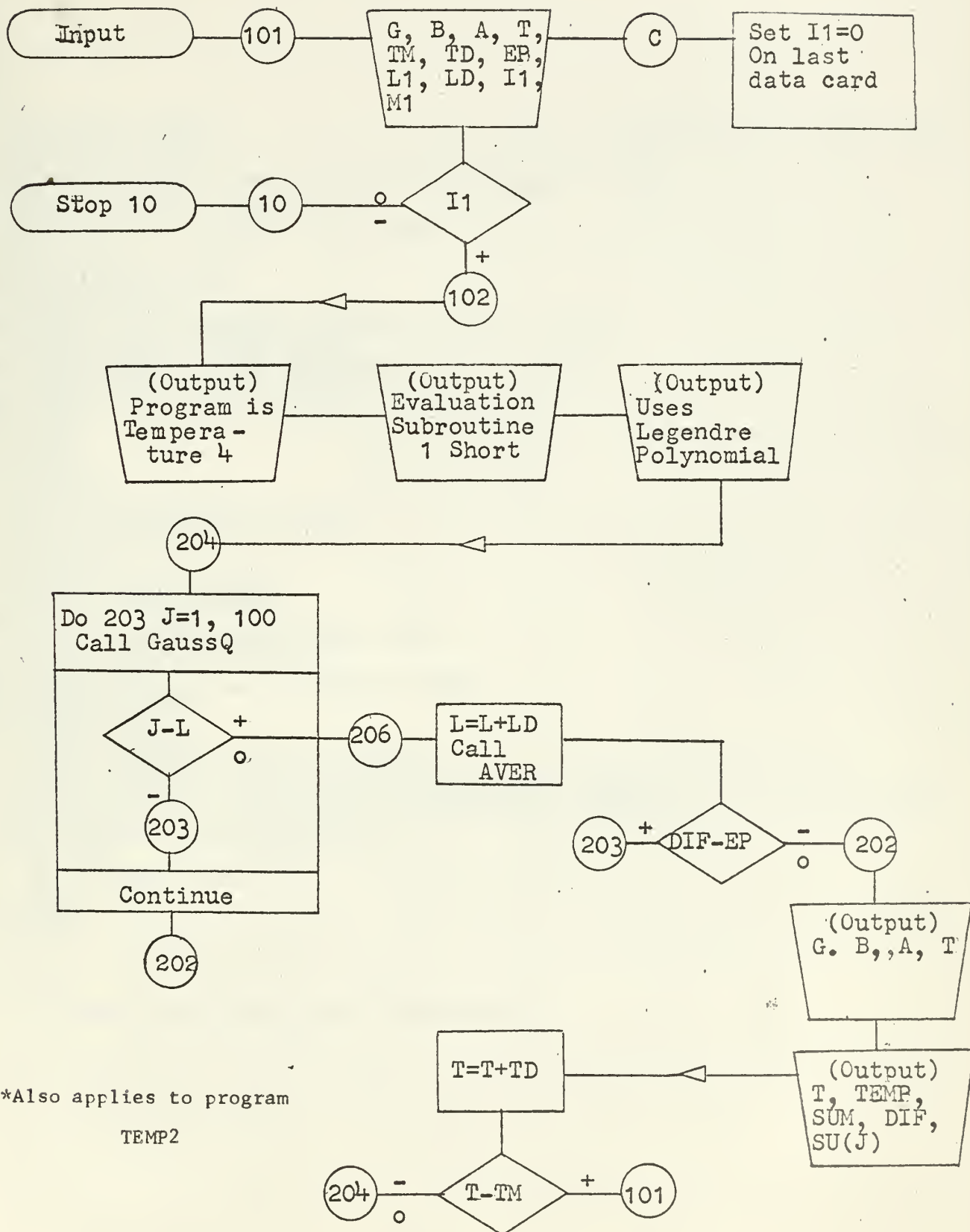


```

PROGRAM SLO4
DIMENSION RR(128),RI(128),VI(20),VR(20),SU(200),AV(12,10),R(129),
1X(129),SLO(10),T(10)
COMMON SLOPE,SLO,T,NT,NT1,NT2,K,EP1,G,B,A,PI,T1,TM
COMMON NT3
101 READ 100,G,B,A,T1,TM,TD,EP,L1,LD,I1
100 FORMAT(7F10.5,3I3)
C SET I1 = 0 ON LAST DATA CARD
IF(I1)10,10,102
102 C1=1.0
210 WRITE OUTPUT TAPE 4,301
301 FORMAT(24H PROGRAM IS SLOPE 4, N=4)
WRITE OUTPUT TAPE 4,304
304 FORMAT(26H USES CHEBYSHEV POLYNOMIAL)
401 WRITE OUTPUT TAPE 4,302
302 FORMAT(30H EVALUATION SUBROUTINE 2S /)
W1C=.10776070/.98480775
W2C=.083333333/.86602540
W3C=.045908434/.64278761
W4C=.012997531/.34202014
NT=-1
NT1=-1
NT2=0
K=1
EP1=.000001
NT3=-1
204 P=3.1415926536/T1
DO 500 I=1,200
500 SU(I)=0.0
L=L1
P1=1./9.
SGN=1.
SU=0.
DO 203 J=1,100
IF(J-1)600,600,601
600 P1=-7./18.
GO TO 603
601 IF(J-2)602,602,603
602 P1=11./18.
603 DO 200 I=1,8
Y=P1*P
CALL SOOTS2 (G,B,A,Y,R,X,RR,RI)
CALL EVAL2S(RR,RI,G,B,Y,C1,VR,VI)
VR(I)=VR
VI(I)=VI
200 P1=P1+(1./9.)
IF(J-1)604,604,605
604 SU(1)=.5*SGN*(W1C*(VR(4)+VR(5))+W2C*(VR(3)+VR(6))+W3C*(VR(2)+VR(7)
1)+W4C*(VR(1)+VR(8)))+SU(J-1)
GO TO 212
605 SU(J)=SGN*(W1C*(VR(4)+VR(5))+W2C*(VR(3)+VR(6))+W3C*(VR(2)+VR(7))+
1W4C*(VR(1)+VR(8)))+SU(J-1)
IF(J-1) 212,212,213
212 PRINT 3,G,B,A,T1
213 CONTINUE
SGN=-SGN
P1=P1+(2./9.)
IF(J-L)203,206,206
206 L=L+LD
CALL AVER(SU,AV,I1,J,DIF,SUM)
IF(DIF-EP)202,202,203
203 CONTINUE
CALL AVER(SU,AV,10,100,DIF,SUM)
202 EG=EXPF(G*T1)
EG2=2.*EG/T1
SLOPE=EG2*SUM
PRINT 4,SUM,DIF,J,SU(J)
PRINT 2,T1,SLOPE
221 CALL SLOMAX
TM1=8.*TM/3.
IF(NT2)406,406,101
406 IF(T1-TM1)204,204,222
222 PRINT 3,G,B,A,T1
2 FORMAT(3H T=F10.5,3X,6HSLOPE=E15.8/)
3 FORMAT(3H G=F10.5,3X,2HB=F10.5,3X,2HA=F10.5,3X,2HT=F10.5/)
4 FORMAT(5H SUM=E15.8,3X,4HDIF=F10.9,3X,3HSU(13,2H)=E15.8/)
GO TO 101
10 STOP 10
END

```


PROGRAM TEMP4*



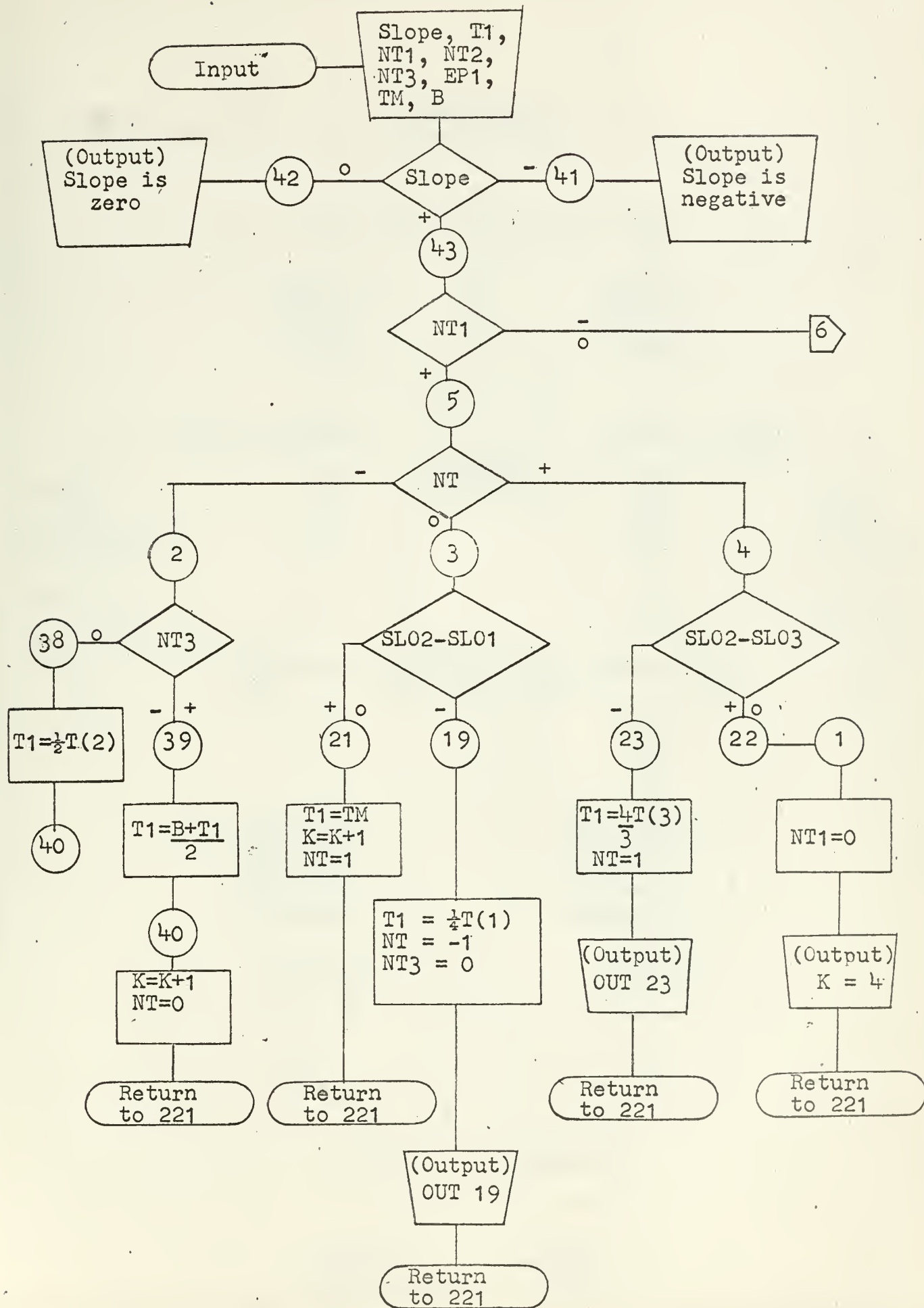
*Also applies to program
TEMP2


```

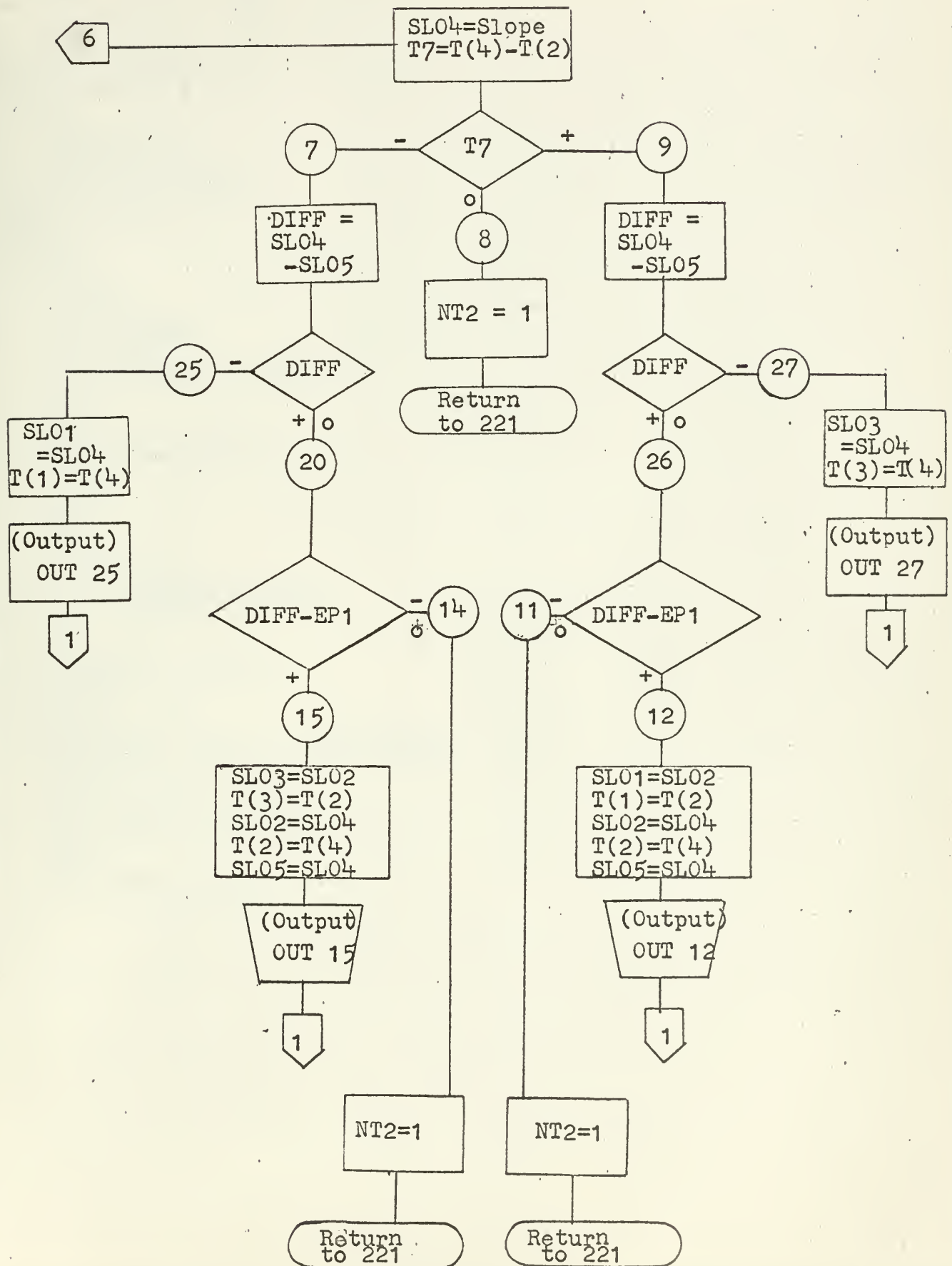
PROGRAM TEMP4*
DIMENSION RR(128),RI(128),VI(20),VR(20),SU(200),AV(12,10),R(129),
1X(129),ER(200)
COMMON G,B,A,T,TM,TD,EP,L1,LD,I1,M1,RR,RI,PI
101 READ 100,G,B,A,T,TM,TD,EP,L1,LD,I1,M1
100 FORMAT(7F10.5,3I3,I1)
SET I1 = 0 ON LAST DATA CARD
IF(I1)10,10,102
102 CONTINUE
PI=3.1415926536
WRITE OUTPUT TAPE 4,300
300 FORMAT(30H PROGRAM IS TEMPERATURE 4, N=8/)
WRITE OUTPUT TAPE 4,302
302 FORMAT(30H EVALUATION SUBROUTINE 1 SHORT/)
WRITE OUTPUT TAPE 4,305
305 FORMAT(25H USES LEGENDRE POLYNOMIAL/)
204 L=L1
L=L1
SU=0.
D=0.0
E=1.0
DO 203 J=1,100
CALL GAUSSQ(D,E,VAL,ER)
D=D+1.0
E=E+1.0
SU(J)=VAL+SU(J-1)
IF(J-L)203,206,206
206 L=L+LD
CALL AVER(SU,AV,I1,J,DIF,SUM)
IF(DIF-EP)202,202,203
203 CONTINUE
CALL AVER(SU,AV, 8,100,DIF,SUM)
202 EG=EXP(-G*T)
EG2=2.*EG/T
TEMP= EG2*SUM
WRITE OUTPUT TAPE 4,1,G,B,A,T
1 FORMAT(3H G=F10.5,3X,2HB=F10.5,3X,2HA=F10.5,3X,2HT=F10.5/)
WRITE OUTPUT TAPE 4,2,T,TEMP,SUM,DIF,J,SU(J)
2 FORMAT(3H T=F10.5,3X,5HTEMP=E20.8,3X,4HSUM=E20.8,3X,4HDIF=F10.9,
13X,3HSU(I3,2H)=E20.8///)
T=T+TD
IF(T-TM)204,204,101
GO TO 101
10 STOP 10
END

```

*TEMP2 is the same except statement 300.



Slomax Subroutine (cont'd)




```

SUBROUTINE SLOMAX
DIMENSION LTITLE(10),RR(128),RI(123),T(10),SLO(10)
COMMON RR,RI,T,SLO,G,B,A,PI,SLOPE,NT,NT1,NT2,EP1,I1,T1
COMMON NT3,TM
IF(SLOPE)41,42,43
41 WRITE OUTPUT TAPE 4,44
44 FORMAT(20H SLOPE 2 IS NEGATIVE/)
GO TO 43
42 WRITE OUTPUT TAPE 4,45
45 FORMAT(26H CALCULATED SLOPE IS ZERO./)
43 IF(NT1)5,6,6
5 IF(NT)2,3,4
2 K=1
T(K)=T1
SLO1=SLOPE
SLO(K)=SLOPE
IF(NT3)39,38,39
38 T1=1.*T(2)/2.
GO TO 40
39 T1=(B+T1)/2.
40 K=K+1
NT=0
RETURN
3 T(K)=T1
SLO2=SLOPE
SLC(K)=SLOPE
SLO5=SLO2
IF(SLO2-SLO1)19,21,21
19 T1=1.*T(1)/4.
NT=-1
NT3=0
PRINT 35
35 FORMAT(7H OUT 19/)
RETURN
21 T1=TM
K=K+1
NT=1
RETURN
4 T(K)=T1
SLO3=SLOPE
IF(SLO2-SLO3)23,22,22
23 T1=4.*T(3)/3.
NT=1
PRINT 36
36 FORMAT(7H OUT 23/)
RETURN
22 SLO(K)=SLOPE
K=K+1
1 C1=SLO1*(T(2)*T(2)-T(3)*T(3))
C2=-SLO2*(T(1)*T(1)-T(3)*T(3))
C3=SLO3*(T(1)*T(1)-T(2)*T(2))
C4=SLO1*(T(2)-T(3))
C5=-SLO2*(T(1)-T(3))
C6=SLO3*(T(1)-T(2))
T1=.5*(C1+C2+C3)/(C4+C5+C6)
NT1=0
PRINT 30,K
30 FORMAT(3H K=I3/)

```



```

        RETURN
6  ER1=0.0
   SLC4=SLOPE
   T(K)=T1
   SLO(K)=SLOPE
   T7=T(4)-T(2)
   IF(T7)7,8,9
7  DIFF=SLO4-SLO5
   IF(DIFF)25,20,20
25 SLO1=SLO4
   SLO(1)=SLO4
   T(1)=T(4)
   PRINT 31
31 FORMAT(7H OUT 25/)
   GO TO 1
20 IF(DIFF-EP1)14,14,15
8  CONTINUE
   NT2=1
   RETURN
9  DIFF=SLO4-SLO5
   IF(DIFF)27,26,26
27 SLC3=SLO4
   SLO(3)=SLO4
   T(3)=T(4)
   PRINT 32
32 FORMAT(7H OUT 27/)
   GO TO 1
26 IF(DIFF-EP1)11,11,12
11 CONTINUE
   NT2=1
   RETURN
12 CONTINUE
   SLO1=SLO2
   SLO(1)=SLO2
   T(1)=T(2)
   SLO2=SLO4
   SLO(2)=SLO4
   T(2)=T(4)
   SLO5=SLO4
   PRINT 33
33 FORMAT(7H OUT 12/)
   GO TO 1
14 CONTINUE
   NT2=1
   RETURN
15 CONTINUE
   SLO3=SLO2
   SLO(3)=SLO2
   T(3)=T(2)
   SLO2=SLO4
   SLO(2)=SLO4
   T(2)=T(4)
   SLO5=SLO4
   PRINT 34
34 FORMAT(7H OUT 15/)
   GO TO 1
END

```



```

SUBROUTINE AVER(S,A,I1,J1,DIF,SUM)
DIMENSION S(200),A(12,1C)
I2=I1+1
N1=J1-I1-1
DO 1 I=1,I2
  A(I,1)=0.5*(S(N1)+S(N1+1))
1 N1=N1+1
  I3=I1-1
  N1=I2
  DO 2 I=1,I3
    N1=N1-1
    DO 2 J=1,N1
      2 A(J,I+1)=0.5*(A(J+1,I)+A(J,I))
      DIF=ABSF((A(N1,I3+1)-A(N1-1,I3+1))/A(N1,I3+1))
      SUM=A(N1,I3+1)
    END
  SUBROUTINE GAUSSQ(D,E,SUM)
  DIMENSION XSI(24),WSI(24),X(9),W(9),RR(128),RI(128),T(10),SLO(10)
  COMMON RR,RI,T,SLO,G,B,A,PI,SLOPE,NT,NT1,NT2,EP1,I1,T1
  IF(W)5,1,5
1 W=1.0
  XSI(16)=0.1834346425
  XSI(17)=0.5255324099
  XSI(18)=0.7966664774
  XSI(19)=0.9602898565
  XSI(20)=0.0
  XSI(21)=0.3242534234
  XSI(22)=0.6133714327
  XSI(23)=0.8360311073
  XSI(24)=0.9681602395
  WSI(16)=0.3626837834
  WSI(17)=0.3137066459
  WSI(18)=0.2223810345
  WSI(19)=0.1012285363
  WSI(20)=0.3302393550
  WSI(21)=0.3123470770
  WSI(22)=0.2606106964
  WSI(23)=0.1806481607
  WSI(24)=0.0812743884
5 N1=8
  I2=19
  I3=N1/2
  K2=I2
  A1=(E+D)*0.5
  A2=(E-D)*0.5
33 I5=N1
  DO 35 I=1,I3
    X(I)=A1-A2*XSI(K2)
    W(I)=A2*WSI(K2)
    X(I5)=A1+A2*XSI(K2)
    W(I5)=W(I)
    K2=K2-1
35 I5=I5-1
49 SUM=0.0
  DO 37 I=1,N1
    X1=X(I)
    CALL EVAL35(X1,VR,VI)
37 SUM=SUM+VI*W(I)
  RETURN
  END

```



```

SUBROUTINE SCOTS2(R,X,Y)
DIMENSION R(129),X(129),RR(128),RI(128),IT(10)
COMMON G,B,A,T,TM,TD,EP,L1,LD,I1,M1,RR,RI,PI
R(1)=1.0
R(2)=B
R(3)=- (B/A)*(G+1.)
R(4)=- ((B**2)/A)*G
X(1)=0.0
X(2)=0.0
X(3)=- (B/A)*Y
X(4)=- ((B**2)/A)*Y
NO=3
MM=0
IT=0
CALL TOOTS2(R,X,NO,IT,MM,-.5,+.5)
IF(RR(1))4,4,5
RRR=0.
RII=0.
5 RRR=RR(1)
RII=RI(1)
RR(1)=RR(2)
RI(1)=RI(2)
RR(2)=RR(3)
RI(2)=RI(3)
RR(3)=RRR
RI(3)=RII
GO TO 3
4 IF(RR(2))3,3,6
6 RRR=RR(2)
RII=RI(2)
RR(2)=RR(3)
RI(2)=RI(3)
RR(3)=RRR
RI(3)=RII
3 RETURN
END

```


For use with SL02 and SL04.

```
SUBROUTINE EVAL2S(RR,RI,G,B,Y,C1,VR,VI)
DIMENSION Z(3),SR(4,4),SI(4,4),E(3),S(3),C(3),RR(128),RI(128),W(3)
DO 100 I=1,3
  Z(I)=(RR(I)*RR(I)-RI(I)*RI(I))/B)+RR(I)
100 W(I)=(2.*RR(I)*RI(I)/B)+RI(I)
DO101 I=1,2
DO102 J=2,3
  SR(I,J)=(Z(I)*Z(J))-(W(I)*W(J))
102 SI(I,J)=(Z(I)*W(J))+(Z(J)*W(I))
101 CONTINUE
E31=EXPF(RR(3)+RR(1))
S31=SINF(RI(3)+RI(1))
C31=COSF(RI(3)+RI(1))
AR1=E31*C31
AI1=E31*S31
E3=EXPF(RR(3))
S3=SINF(RI(3))
C3=COSF(RI(3))
DR1=E3*C3
DI1=E3*S3
E1=EXPF(RR(1))
S1=SINF(RI(1))
C1=COSF(RI(1))
ER1=E1*C1
EI1=E1*S1
SRN=SR(2,3)-SR(1,2)
SIN=SI(2,3)-SI(1,2)
SRD1=SR(2,3)-SR(1,3)
SID1=SI(2,3)-SI(1,3)
SRD2=SR(1,3)-SR(1,2)
SID2=SI(1,3)-SI(1,2)
ANR=(SRN*AR1)-(SIN*AI1)
ANI=(SIN*AR1)+(SRN*AI1)
DNR1=SRD1*DR1-SID1*DI1
DNI1=SID1*DR1+SRD1*DI1
DNR2=SRD2*ER1-SID2*EI1
DNI2=SID2*ER1+SRD2*EI1
DNR=DNR1+DNR2
DNI=DNI1+DNI2
ANUR=ANR*DNR+ANI*DNI
ANUI=ANI*DNR-ANR*DNI
DENOM=DNR*DNR+DNI*DNI
VR=C1*(ANUR/DENOM)
VI=C1*(ANUI/DENOM)
END
```



```

SUBROUTINE EVAL2L(RR,RI,G,B,Y,C1,VR,VI)
DIMENSION Z(3),SR(4,4),SI(4,4),E(3),S(3),C(3),RR(128),RI(128),W(3)
DO100 I=1,3
Z(I)=((RR(I)**2-RI(I)**2)/B)+RR(I)
100 W(I)=(2.*RR(I)*RI(I)/B)+RI(I)
DO101 I=1,2
DO102 J=2,3
SR(I,J)=(Z(I)*Z(J))-(W(I)*W(J))
102 SI(I,J)=(Z(I)*W(J))+(Z(J)*W(I))
101 CONTINUE
E31=EXPF(RR(3)+RR(1))
S31=SINF(RI(3)+RI(1))
C31=COSF(RI(3)+RI(1))
E32=EXPF(RR(3)+RR(2))
S32=SINF(RI(3)+RI(2))
C32=COSF(RI(3)+RI(2))
E21=EXPF(RR(2)+RR(1))
C21=COSF(RI(2)+RI(1))
S21=SINF(RI(2)+RI(1))
DO 103 I=1,3
E(I)=EXPF(RR(I))
S(I)=SINF(RI(I))
103 C(I)=COSF(RI(I))
AR1=E31*C31
AI1=E31*S31
AR2=E21*C21
AI2=E21*S21
BR1=AR2

BI1=AI2
BR2=E32*C32
BI2=E32*S32
CR1=BR2
CI1=BI2
CR2=AR1
CI2=AI1
AR12=AR1-AR2
AI12=AI1-AI2
A1R=(SR(2,3)*AR12)-(SI(2,3)*AI12)
A1I=(SI(2,3)*AR12)+(SR(2,3)*AI12)
DR1=E(3)*C(3)
DI1=E(3)*S(3)
DR2=E(2)*C(2)
DI2=E(2)*S(2)
DR12=DR1-DR2
DI12=DI1-DI2
ER1=E(1)*C(1)
EI1=E(1)*S(1)
ER2=DR1
EI2=DI1
ER12=ER1-ER2
EI12=EI1-EI2
FR1=DR2
FI1=DI2
FR2=ER1
FI2=EI1
FR12=FR1-FR2
FI12=FI1-FI2
BR12=BR1-BR2
BI12=BI1-BI2
CR12=CR1-CR2
CI12=CI1-CI2
B2R=(SR(1,3)*BR12)-(SI(1,3)*BI12)
B2I=(SI(1,3)*BR12)+(SR(1,3)*BI12)
C3R=(SR(1,2)*CR12)-(SI(1,2)*CI12)
C3I=(SI(1,2)*CR12)+(SR(1,2)*CI12)
D1R=(SR(2,3)*DR12)-(SI(2,3)*DI12)
D1I=(SI(2,3)*DR12)+(SR(2,3)*DI12)
E2R=(SR(1,3)*ER12)-(SI(1,3)*EI12)
E2I=(SI(1,3)*ER12)+(SR(1,3)*EI12)
F3R=(SR(1,2)*FR12)-(SI(1,2)*FI12)
F3I=(SI(1,2)*FR12)+(SR(1,2)*FI12)
ANR=A1R+B2R+C3R
ANI=A1I+B2I+C3I
DNR=D1R+E2R+F3R
DNI=D1I+E2I+F3I
ANUR=ANR*DNR+ANI*DNI
ANUR=ANR*DNR+ANI*DNI
ANUI=ANI*DNR-ANR*DNI
ANUI=ANI*DNR-ANR*DNI
DENOM=DNR*DNR+DNI*DNI
DENOM=DNR*DNR+DNI*DNI
VR=C1*(ANUR/DENOM)
VI=C1*(ANUI/DENOM)
END

```

For use with SLO2 and SLO4
when NTU less than 5

For use with TEMP2 and TEMP4

```

SUBROUTINE EVAL53S(X1,VR,VI)
  DIMENSION Z(3),SR(4,4),SI(4,4),E(3),S(3),C(3),RR(128),RI(128),W(3)
  1,R(129),X(129)
  COMMON G,B,A,T,TM,TD,EP,L1,LD,I1,N1,RR,RI,PI
  Y=(PI/T)*X1
  CALL SOOTS2(R,X,Y)
  C1=1.0
  DO 100 I=1,3
    Z(I)=((RR(I)*RR(I)-RI(I)*RI(I))/B)+RR(I)
  100 W(I)=(2.*RR(I)*RI(I)/B)+RI(I)
  DO101 I=1,2
  DO102 J=2,3
  102 SR(I,J)=(Z(I)*Z(J))-(W(I)*W(J))
  101 SI(I,J)=(Z(I)*W(J))+(Z(J)*W(I))
  CONTINUE
  E31=EXPF(RR(3)+RR(1))
  S31=SINF(RI(3)+RI(1))
  C31=COSE(RI(3)+RI(1))
  AR1=E31*C31
  AI1=E31*S31
  E3=EXPF(RR(3))
  S3=SINF(RI(3))
  C3=COSE(RI(3))
  DR1=E3*C3
  DI1=E3*S3
  E1=EXPF(RR(1))
  S1=SINF(RI(1))
  C11=COSE(RI(1))
  ER1=E1*C11
  EI1=E1*S1
  SRN=SR(2,3)-SR(1,2)
  SIN=SI(2,3)-SI(1,2)
  SRD1=SR(2,3)-SR(1,3)
  SID1=SI(2,3)-SI(1,3)
  SRD2=SR(1,3)-SR(1,2)
  SID2=SI(1,3)-SI(1,2)
  ANR=(SRN*AR1)-(SIN*AI1)
  ANI=(SIN*AR1)+(SRN*AI1)
  DNR1=SRD1*DR1-SID1*DI1
  DNI1=SID1*DR1+SRD1*DI1
  DNR2=SRD2*ER1-SID2*EI1
  DNI2=SID2*ER1+SRD2*EI1
  DNR=DNR1+DNR2
  DNI=DNI1+DNI2
  DENR=(G*DNR)-Y*DNI
  DENI=(Y*DNR)+G*DNI
  DENOM=(DENR*DENR)+DENI*DENI
  VR=C1*COSE(PI*X1)*(ANR*DENR+ANI*DENI)/DENOM
  VI=-C1*SINF(PI*X1)*(ANI*DENR-ANR*DENI)/DENOM
  END

```


For use with SLO3 and SLO5, $\alpha = 0$.

```
SUBROUTINE EVAL35(X1,VR,VI)
DIMENSION VR(20),VI(20),SU(200),AV(12,10),R(129),X(129),ER(200),
1RR(128),RI(128),T(10),SLO(10)
COMMON RR,RI,T,SLO,G,B,A,PI,SLOPE,NT,NT1,NT2,EP1,I1,T1
COMMON NT3,TM
Y=(PI/T1)*X1
C1=1.
D1=((G*G)+G+(Y*Y))/((G+1.)*(G+1.)+(Y*Y))
E1=EXP(-B*D1)
F=Y/((G+1.)*(G+1.)+(Y*Y))
C=COF(B*F)
S=SINF(B*F)
VR=C1*E1*C*COF(PI*X1)
VI=C1*E1*S*SINF(PI*X1)
END
END
```

For use with TEMP2 and TEMP4, $\alpha = 0$

```
SUBROUTINE EVAL3T(X1,VR,VI)
DIMENSION Z(3),SR(4,4),SI(4,4),E(3),S(3),C(3),RR(128),RI(128),W(3)
1,R(129),X(129)
COMMON G,B,A,T,TM,TD,EP,L1,LD,I1,M1,RR,RI,PI
Y=(PI/T)*X1
C1=1.0
G1=G+1.
DEN=G1*G1+Y*Y
D1=(G*G+Y*Y)/DEN
F1=(G1*Y-G*Y)/DEN
E1=EXP(-B*D1)
C=COF(B*F1)
S=SINF(B*F1)
DENOM=G*G+Y*Y
VR=C1*COF(PI*X1)*E1*(C*G+S*Y)/DENOM
VI=C1*SINF(PI*X1)*E1*(S*G-C*Y)/DENOM
END
```


thesM8217

Solution of the single blow problem with



3 2768 001 91661 2

DUDLEY KNOX LIBRARY